



Townsend, Alexandra J. and Retkute, Renata and Chinnathambi, Kannan and Randall, Jamie W.P. and Foulkes, John F and Carmo-Silva, Elizabete and Murchie, Erik H. (2017) Suboptimal acclimation of photosynthesis to light in wheat canopies. *Plant Physiology* . ISSN 1532-2548 (In Press)

**Access from the University of Nottingham repository:**

<http://eprints.nottingham.ac.uk/48834/1/townsend%20et%20al%202017.pdf>

**Copyright and reuse:**

The Nottingham ePrints service makes this work by researchers of the University of Nottingham available open access under the following conditions.

This article is made available under the University of Nottingham End User licence and may be reused according to the conditions of the licence. For more details see:  
[http://eprints.nottingham.ac.uk/end\\_user\\_agreement.pdf](http://eprints.nottingham.ac.uk/end_user_agreement.pdf)

**A note on versions:**

The version presented here may differ from the published version or from the version of record. If you wish to cite this item you are advised to consult the publisher's version. Please see the repository url above for details on accessing the published version and note that access may require a subscription.

For more information, please contact [eprints@nottingham.ac.uk](mailto:eprints@nottingham.ac.uk)

1 **Short Title:** Suboptimal photosynthetic acclimation in wheat

2

3 **Corresponding Author:** Alexandra J Townsend,

4 alexandra.townsend@nottingham.ac.uk

5 Tel: +44 (0)115 951 6234

6 **Suboptimal acclimation of photosynthesis to light in wheat canopies**

7 **Alexandra J Townsend<sup>1,2\*</sup>, Renata Retkute<sup>1,3</sup>, Kannan Chinnathambi<sup>1</sup>, Jamie WP**

8 **Randall<sup>1</sup>, John Foulkes<sup>1</sup>, Elizabete Carmo-Silva<sup>4</sup> and Erik H Murchie<sup>1</sup>**

9

10 **Addresses**

11 <sup>1</sup>Division of Plant and Crop Science, School of Biosciences, University of Nottingham,

12 Sutton Bonington Campus, LE12 5RD, UK

13 <sup>2</sup>Crops for The Future, Jalan Broga, 43500 Semenyih Selangor Darul Ehsan, Malaysia.

14 <sup>3</sup>School of Life Sciences, Gibbet Hill Campus, The University of Warwick, Coventry,

15 CV4 7AL

16 <sup>4</sup>Lancaster Environment Centre, Lancaster University, Lancaster, LA1 4YQ, UK

17 \*Alexandra J Townsend Present address: School of Biological and Chemical Sciences,

18 Queen Mary University of London, UK

19

20 **Author Contributions:** A.J.T., R.R. and E.H.M. conceived the original screening and  
21 research plans; E.H.M. and J.F. supervised the experiments; A.J.T. performed most of  
22 the experiments with assistance from K.C. and J.W.P.R; E.C.-S. carried out rubisco  
23 assays and analysis.; A.J.T. and R.R. designed the modelling experiments and analysed  
24 the data; A.J.T. wrote the article with contributions of all the authors; E.H.M.  
25 supervised and made a substantial contribution to the writing.

26 **Funding**

27 This project was funded by the Biotechnology and Biological Sciences Research  
28 Council BBSRC [grant BB/J003999/1]. A.J.T. received funding from Crops for the  
29 Future under project BioP1-006 and the School of Biosciences, University of

30 Nottingham. The wheat BC<sub>3</sub> lines were developed as part of BBSRC [grant  
31 BB/D008972].

32 **One Sentence Summary:** High-resolution 3D reconstruction and ray tracing combined  
33 with an empirical model of photosynthesis reveals sub-optimal photosynthetic  
34 acclimation in wheat canopies.

35

## 37 **Abstract**

38     Photosynthetic acclimation (photoacclimation) is the process whereby leaves alter  
39     their morphology and/or biochemistry to optimise photosynthetic efficiency and  
40     productivity according to long-term changes in the light environment. Three-  
41     dimensional (3D) architecture of plant canopies impose complex light dynamics, but the  
42     drivers for photoacclimation in such fluctuating environments are poorly understood. A  
43     technique for high-resolution 3D reconstruction was combined with ray tracing to  
44     simulate a daily time course of radiation profiles for architecturally contrasting field-  
45     grown wheat canopies. An empirical model of photoacclimation was adapted to predict  
46     the optimal distribution of photosynthesis according to the fluctuating light patterns  
47     throughout the canopies. Whilst the photoacclimation model output showed good  
48     correlation with field-measured gas exchange data at the top of the canopy, it predicted  
49     a lower optimal light saturated rate of photosynthesis ( $P_{max}$ ) at the base. Leaf Rubisco  
50     and protein content were consistent with the measured  $P_{max}$ . We conclude that although  
51     the photosynthetic capacity of leaves is high enough to exploit brief periods of high  
52     light within the canopy (particularly towards the base), the frequency and duration of  
53     such sunflecks are too small to make acclimation a viable strategy in terms of carbon  
54     gain. This suboptimal acclimation renders a large portion of residual photosynthetic  
55     capacity unused, and reduces photosynthetic nitrogen use efficiency (PNUE) at the  
56     canopy level with further implications for photosynthetic productivity. It is argued that  
57     (a) this represents an untapped source of photosynthetic potential and (b) canopy  
58     nitrogen could be lowered with no detriment to carbon gain or grain protein content.

59

## 60 **Key Words**

61     3D reconstruction, Canopy, Model, Nitrogen use efficiency, Photoacclimation,  
62     Photosynthesis, *Triticum aestivum* (Wheat)

## 63    **Introduction**

64     The arrangement of plant material in time and space can result in a heterogeneous and  
65     temporally unpredictable light environment. This is especially true within crop  
66     canopies, where leaf and stem architectural features can lead to complex patterns of  
67     light according to solar movement, weather and wind. This is likely to influence  
68     productivity because photosynthesis is highly responsive to changes in light intensity  
69     over short timescales (seconds to minutes). Leaf photosynthesis does not respond  
70     instantaneously to a sudden change in light level: the delay before steady state is  
71     reached is closely linked to the photosynthetic induction state, which is a physiological  
72     condition dependent on the leaf's recent 'light history' (Sassenrath-Cole and Pearcy  
73     1994, Stegeman et al., 1999). Induction state is defined by factors including the  
74     activation state of photosynthetic enzymes (Yamori et al., 2012; Carmo-Silva and  
75     Salvucci, 2013), stomatal opening (Lawson and Blatt, 2014) and photoprotection  
76     (Hubbart et al., 2012). Together these determine the speed with which a leaf can  
77     respond to an increase, or decrease, in light intensity. It is thought that these processes  
78     are not always coordinated for optimal productivity in fluctuating light, as shown by the  
79     slow recovery of quantum efficiency for CO<sub>2</sub> assimilation ( $\phi$ CO<sub>2</sub>) in low light (Zhu et  
80     al., 2004), high non-photochemical quenching (NPQ) during induction (Hubbart et al.,  
81     2012; Kromdijk et al., 2016) and slow stomatal opening and closure (Lawson and Blatt,  
82     2014). It is predicted that such slow responses of photosynthesis to the environment can  
83     have a substantial impact on wheat yield (Taylor and Long, 2017).

84  
85     The role of light-dependent changes in crop canopies has not had sufficient attention.  
86     Acclimation of photosynthesis to changes in light intensity and quality (here termed  
87     photoacclimation in order to distinguish it from acclimation to other environmental  
88     factors) is the process by which plants alter their structure and composition over long  
89     time periods (days and weeks), in response to the environment they experience.  
90     Photoacclimation can be broadly split into two types: photoacclimation that is  
91     determined during leaf development, including cell size and number plus leaf shape  
92     (Weston et al., 2000; Murchie et al., 2005) or photoacclimation that can occur within  
93     mature tissues (Anderson et al., 1995; Walters, 2005; Retkute et al., 2015). Whilst the  
94     former is largely irreversible, the latter, here termed dynamic photoacclimation, can be  
95     reversible. Differences include changes in light harvesting capacity (shown by  
96     chlorophyll a:b ratio), chlorophyll per unit nitrogen (N), electron transport capacity per

unit chlorophyll and rate of electron transport capacity relative to Rubisco activity (Björkman, 1981; Evans, 1989; Evans and Poorter, 2001). This involves change in relative amounts of a number of primary components and processes, including light harvesting pigment protein complexes (LHC), Calvin cycle enzymes and electron transport components such as the cytochrome b/f complex. It is normally considered that photoacclimation represents an economy of form and function, permitting higher capacity for carbon assimilation in high light whilst improving the quantum efficiency at low light (Björkman, 1981; Anderson and Osmund, 1987; Anderson et al., 1995; Murchie and Horton, 1997). This gives rise to the further concept that the plant must measure and predict changes in its environment to elicit the most efficient response. It is known that photoacclimation responses to fluctuating light can be complex (Viale-Chabrand *et al.*, 2017) and that disruption of photoacclimation using mutants of *Arabidopsis thaliana* results in a loss of fitness (Athanasίου et al., 2010).

Is photoacclimation optimised for crop canopies? It is assumed to improve productivity because, following long-term shifts in light intensity, it permits a higher rate of photosynthesis at high light and a higher quantum efficiency at low light. Over time this will directly influence the ability of the canopy to ‘convert’ intercepted radiation to biomass and grain yield and reduce the amount of absorbed solar energy in potentially ‘wasteful’ processes such as non-photochemical quenching (Zhu et al 2010; Murchie and Reynolds, 2012; Kromdijk et al., 2016). However, this has never been empirically tested in crop canopies which often possess complex light dynamics that are dependent on architecture (Burgess et al., 2015). Hence, we do not know which features of photoacclimation would make appropriate traits for crop improvement.

To solve this problem, we need to first understand the features of natural light that trigger photoacclimation e.g. integrated light levels, duration of high - low light periods or the frequency of high - low light periods. Early work suggested that integrated PPFD could be an important driver (Chabot et al., 1979; Watling et al., 1997), however later work, using well characterised artificial fluctuations, highlighted the importance of the duration of high and low light periods (Yin and Johnson, 2000; Retkute et al., 2015). It therefore follows that the precise characteristics of the light environment are important when determining if photoacclimation is operating in a manner that maintains fitness and productivity. Past theoretical work has tended to focus upon canopies with randomly distributed leaves in space (Werner et al., 2001; Zhu et al., 2004) with few

132 recent models using more complex and realistic architectural features (Song et al., 2013;  
133 Burgess et al., 2015). This necessitates the study of photoacclimation in the context of  
134 light dynamics within accurately reconstructed 3-dimensional plant canopies because  
135 even moderate changes in architecture can have a large impact on light characteristics  
136 (Burgess et al., 2015). Photoacclimation to high light requires an energy source and  
137 resources (carbon (C), nitrogen (N) and others) in order to enhance, for example,  
138 Rubisco per unit leaf area. It can be argued that a high light saturated photosynthetic  
139 capacity ( $P_{max}$ ) is advantageous under low light because it enables the exploitation of  
140 high light periods (sunflecks). However, maintenance of a thick high-light acclimated  
141 leaf with a high  $P_{max}$  (and high chlorophyll) may impose a respiratory burden and  
142 influence the efficiency of photosynthesis under low light. The advantage of  
143 maintaining a high  $P_{max}$  then becomes dependent on the frequency and duration of high  
144 sunflecks in the canopy and how fast photosynthetic induction can occur in response to  
145 each fleck. Although this question has been addressed to an extent in the ecological  
146 literature (e.g. Hikosaka, 2016) it is still not known whether there is an advantage to  
147 maintaining a higher  $P_{max}$  lower in the crop canopy in order to exploit sunflecks  
148 (Pearcy, 1990), or whether architecture influences the potential gain. Again, it depends  
149 on knowing the precise 3D pattern or light over time and predicting its likely effect on  
150 photoacclimation.

151

152 A last consideration concerns how photoacclimation is influenced by phenology and  
153 physiology within the canopy. In a cereal such as wheat, development occurs initially in  
154 high light, followed by progressive shading by younger leaves. Hence it might be  
155 expected that photoacclimation would track this change in light accurately. However,  
156 the photosynthetic system represents a significant sink for leaf N and other soil-derived  
157 mineral elements and this sink will increase in size as photosynthetic capacity of the  
158 leaf rises. It has been suggested that lower leaves in the canopy act as a functional  
159 reserve of minerals such as N. This may also lead to retention of a high  $P_{max}$  (Murchie et  
160 al., 2002; Sinclair and Sheehy, 1999). Lower leaves contribute relatively little to grain  
161 yield during grain filling (approximately 3% of light interception in leaf 4 at anthesis),  
162 thus optimising photoacclimation in flag leaf and second leaf will be the main targets  
163 for yield potential gains, whilst leaf 3 and 4 will be the main targets for gains in  
164 photosynthesis per unit N (PNUE). Although a decline in photosynthesis generally  
165 corresponds to the change in light during canopy development, there is variation in this  
166 relationship according to species (Hikosaka 2016). The extent of optimality of

167 photoacclimation (in isolation from other factors) depends on the exact sequence,  
168 frequency and duration of high light fluctuations of light within the canopy. The latter  
169 is unknown for realistic canopy light fluctuations. In other words, is it economically  
170 viable for a leaf to acclimate to high light in order to exploit brief periods of high light  
171 (Pearcy 1990)? We define optimality as that condition which results in the highest  
172 carbon gain for a given fluctuating light environment.

173

174 To address these questions, we have developed two novel techniques. First, a model  
175 of photoacclimation that provides a quantitative indicator of carbon gain, predicting  
176 optimal maximal photosynthetic capacity levels ( $P_{max}^{opt}$ ) for a given variable environment  
177 (Retkute et al., 2015). Second, a method for the 3-dimensional (3D) high-resolution  
178 reconstruction of plant canopies without the need to parameterise structural models that,  
179 with available ray tracing techniques (Song et al., 2013), can characterise light in every  
180 point in the canopy over the course of a day (Pound et al., 2014; Burgess et al., 2015).  
181 This allows precise canopy architecture to be considered and a profile of light intensities  
182 for any part of the canopy throughout the day to be produced. Here we use these  
183 techniques in combination with manual measurements of photosynthesis to predict the  
184 optimal photoacclimation status (to light alone) throughout canopy depth according to  
185 the (variable) light environment determined by contrasting canopy architectures. We  
186 show that the  $P_{max}$  value optimised for light in all leaves in the bottom canopy layers is  
187 substantially lower than that measured, an observation that has implications for PNUE  
188 of the whole canopy and questions the common assumption that an accumulation of  
189 Rubisco at lower canopy positions allows exploitation of sunflecks.





## 191   **Results**

### 192   *The Canopy Light Environment*

193     Fig. 1 shows an example of the reconstruction process whilst Fig. 2 shows the final  
194     six canopies (three per growth stage) used within this study. The wheat lines selected  
195     were the same as those used for a previous study (Burgess et al., 2015) and chosen due  
196     to their contrasting architectural features. The Parent line (Ashby) contains more upright  
197     leaves, Line 2 (cv 23-74) more curled leaves and Line 1 (cv 32-129) with an  
198     intermediate phenotype (see materials and methods for more details on the wheat lines  
199     studied). Similar features were observed as in Burgess et al. (2015) except for a more  
200     curled leaf phenotype of Line 1 relative to the previous year, slightly increased plant  
201     height and altered Leaf Area Index (LAI; leaf area per unit ground area: see Table 1 and  
202     2; measured physical plant measurements and reconstruction LAI values). Burgess et al.  
203     (2015) showed that manually measured leaf area corresponded well to reconstructed  
204     values. Here we find that LAI was slightly higher in all the reconstructions compared to  
205     the measured values, which was likely due to differences in the way in which stem and  
206     leaf area is accounted for in each method. In particular, the manual method did not  
207     account for all stem material (some was too large for the leaf area analyser) and the  
208     reconstruction method slightly over estimated stem area. This overestimation was  
209     consistent for all lines. Plant density, tillering and plant height were equivalent in Lines  
210     1 and 2 but slightly higher in the Parent line (Table 1). Further architectural  
211     characteristics of the three contrasting lines are given in Supplementary Table S1.

212

213     Simulations of the light environment within each of the canopies indicate that the  
214     daily photosynthetic photon flux density (PPFD) decreases with depth in all three plots  
215     at both growth stages, however there is considerable heterogeneity at each depth that  
216     needs to be accounted for in the model application. Fig. 3 shows how PPFD varies with  
217     depth in three randomly selected triangles at each of the three depth positions where  
218     samples for rubisco measurements were taken and where gas exchange measurements  
219     were made. The progressive lowering in the canopy position also leads to more  
220     infrequent periods of high light intensity, or sunflecks, interspersed with periods of low  
221     light intensity, approaching the critical value for positive net photosynthesis (see  
222     below). Similar light signatures are seen for all canopies and both growth stages studied  
223     (data not shown). To validate the predicted light levels in each of the canopies using ray  
224     tracing, the modelled data were compared to manual measurements taken in the field

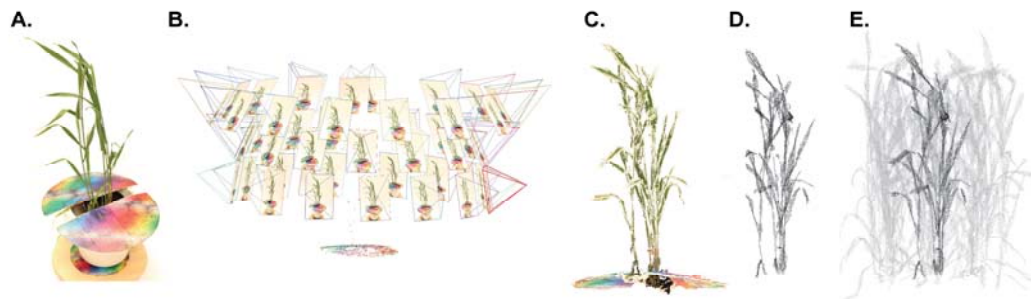


**Figure 1.** Overview of the reconstruction process **A.** original photograph, **B.** point cloud reconstruction using stereocameras (Wu, 2011), **C.** output point cloud, **D.** mesh following reconstruction method (Pound et al., 2014) and **E.** final canopy reconstruction. N.B. The multi-coloured disc in panels A-C is a calibration target, used to optimise the reconstruction process and scale the final reconstructions back to their original units.

225 with a ceptometer as the logarithm of the ratio of light received on a horizontal surface  
 226 and light intercepted by a point on the leaf ( $\text{Ln}[L/L_0]$ ; Supplementary Fig. S1).  
 227

#### 228 ***Disparity between modelled and measured $P_{max}$ at the bottom of the canopy***

229 Fig. 4 shows light response curves of photosynthesis for each of the lines at three  
 230 canopy levels. Typical responses are seen: a decline in both  $P_{max}$  and dark respiration  
 231 rate with increasing canopy depth. A significant lowering of  $P_{max}$  was observed within  
 232 the two lower layers at postanthesis. A comparison of photosynthesis rates with light  
 233 levels (Fig. 3) shows that all leaves would remain above the light compensation point  
 234 and positively contribute to carbon gain.

235  
 236 An empirical model of photoacclimation was applied (see Retkute et al., 2015 and  
 237 materials and methods) to predict the optimal  $P_{max}$  ( $P_{max}^{opt}$ ) for 250 canopy positions. The  
 238 model includes a time weighted average ( $\tau$ ); a calculation of the effect of a variable  
 239 induction state which manifests as a gradually ‘fading memory’ of a high light event  
 240 (see Materials and Methods: Modelling). The average is applied to the transition from  
 241 low to high light (but not high to low) to effectively account for induction state which is  
 242 very difficult to measure *in situ*, and not possible for all points in the canopy, as it  
 243 reflects the past light history of the leaf. Within the main experiment of this study,  $\tau$  was  
 244 set at 0.2, which is equivalent to a maximum leaf memory of around 12 minutes, and is  
 245 in line with previous studies and fit with past experimental data (Percy and Seemann,  
 246 1990; Retkute et al., 2015). The effect of this time weighted average is given in  
 247 Supplementary Fig S2. Fig. 5 shows the result of the modelled  $P_{max}^{opt}$  against measured  
 248  $P_{max}$ . Strikingly, the measured  $P_{max}$  was substantially higher than predicted except in the  
 249 upper parts of the canopy, which showed good correspondence. This was consistently

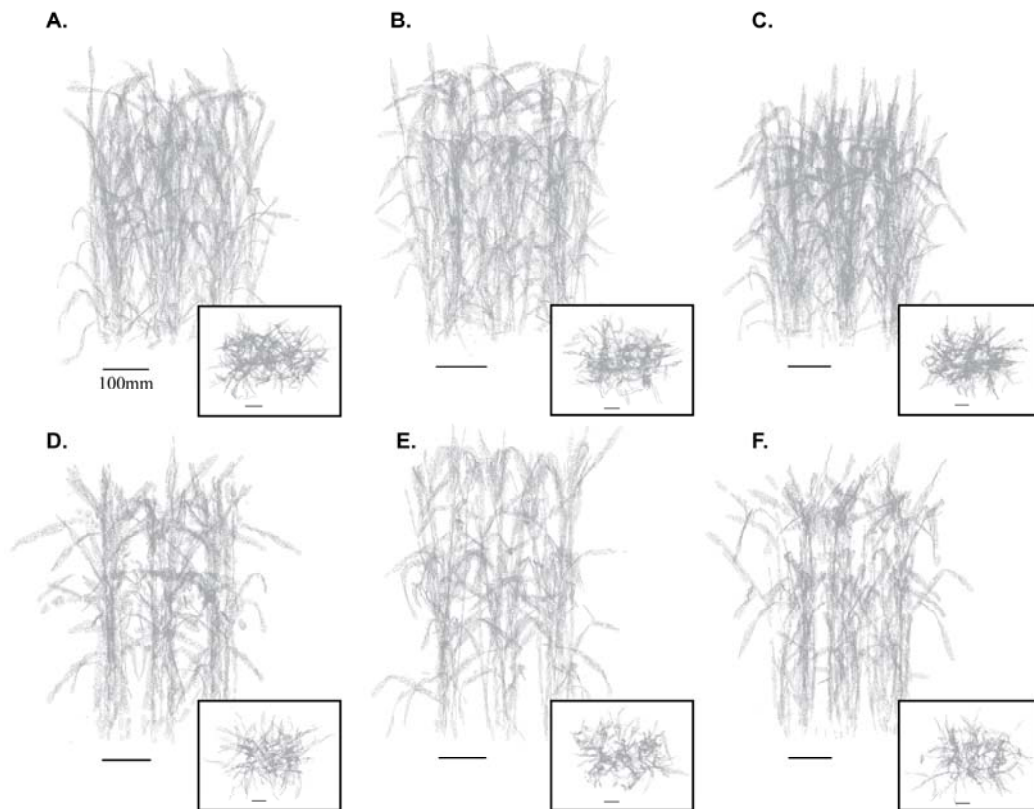


**Figure 2.** Example Canopy Reconstructions from front and top down views. **A-C.** Preanthesis and **D-F.** Postanthesis. **A, D.** Parent Line, **B, E.** Line 1 and **C, F.** Line 2

the case for all lines at both growth stages. In the lowest canopy positions (below 300 mm from the ground) the measured values of  $P_{max}$  were several times higher than the lowest predicted values:  $1 - 2 \mu\text{mol CO}_2 \text{ m}^{-2} \text{ s}^{-1}$ . In these positions the important features were those that support a positive carbon gain in extremely low light environments notably a very low dark respiration level (measured at less than  $0.5 \mu\text{mol m}^{-2} \text{ s}^{-1}$ ) and light compensation point. In other words, the measured  $P_{max}$  would rarely be achieved *in situ* largely due to the brevity of the high light periods and the slow induction of photosynthesis. A comparison with Fig. 3 shows that light levels in this part of the canopy were extremely low:  $10 - 30 \mu\text{mol m}^{-2} \text{ s}^{-1}$  punctuated by rare short lived high light events with a large variation in frequency and intensity. The decay of modelled  $P_{max}^{opt}$  was exponential (Fig. 5) consistent with that of light (Hirose, 2005) in contrast with the measured  $P_{max}$  which appeared linear. It was also notable that the different canopy architectures (analysed in Burgess et al., 2015 which used the same set of lines) were associated with similar disparity between measured and modelled levels of photosynthesis. However, this difference was greater in Line 2 (non-erect leaves) which had a higher rate of light extinction. A comparison of the modelled and measured  $P_{max}$  versus PPFD at 12:00 h, plus modelled  $P_{max}^{opt}$  versus daily PPFD is given in

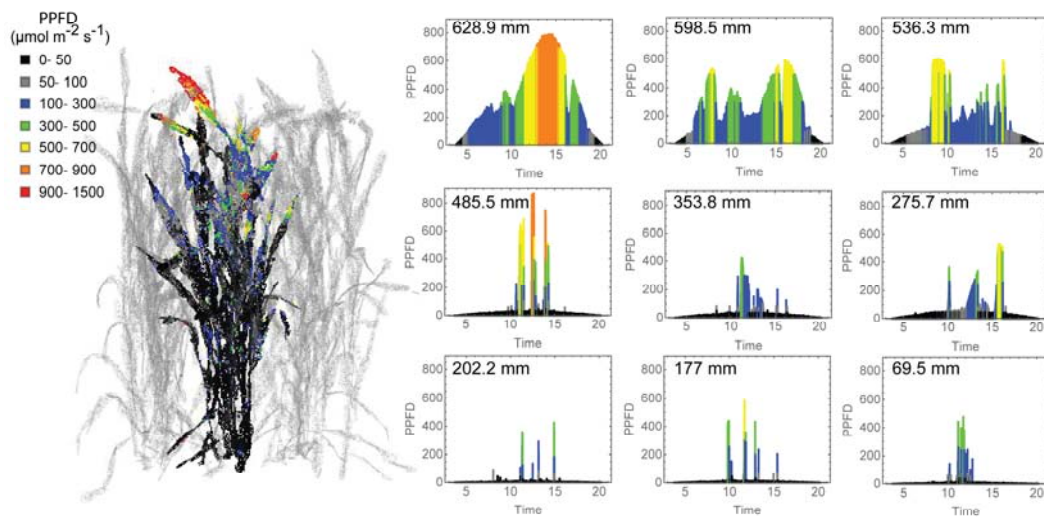


**Figure 3.** Progressive lowering of the canopy position in a canopy results in a reduction in daily integrated PPFD ( $\mu\text{mol m}^{-2} \text{s}^{-1}$ ) but also the pattern and incidence of high light events within the canopy. The left hand panel shows a representative reconstructed preanthesis wheat canopy with a single plant in bold: Maximum PPFD ranges are colour coded. The right hand panels show PPFD during the course of a day at 9 representative and progressively lower canopy positions (the height of each canopy location from the ground given in the top left corner of each graph) calculated using ray tracing techniques.

267 Supplementary Fig. S3. This shows a similar spread of modelled versus measured  $P_{max}$   
 268 values and a linear relationship between modelled  $P_{max}^{opt}$  and daily PPFD. We also  
 269 tested the model at a substantially lower value of  $\tau$  (0.1, equivalent to a leaf memory of  
 270 6 minutes; Supplementary Fig. S4), which results in a more rapid response to light  
 271 flecks. Even using this parameter, the  $P_{max}$  was substantially over estimated in the  
 272 bottom layer of the canopy. A sensitivity analysis was performed based around the  
 273 assumption of respiration being proportional to photosynthesis versus respiration having  
 274 a linear relationship with respect to  $P_{max}$  (not allowing  $R_d$  vs  $P_{max}$  to pass through the  
 275 origin). First, two lines were fitted to all measured data, and then we varied  $\alpha$  by +/-  
 276 10%. In both cases changes in predicted  $P_{max}$  for light patterns at different layers in the  
 277 canopy changed by less than 9% and could not account for the disparity between  
 278 modelled and measured data.  
 279

### 280 ***Rubisco and protein content reflect measured, and not modelled, data***

281 During canopy development wheat leaves will normally emerge into high light and  
 282 then become progressively more shaded by production of subsequent leaves. The higher  
 283 than expected measured  $P_{max}$  at the base of the canopy indicates retention of  
 284 components of photosynthesis to a level that was excessive when compared to the  
 285 prevailing light environment. The difference between measured and modelled  $P_{max}$   
 286 became progressively lower, moving from the bottom of the canopy to the top, until

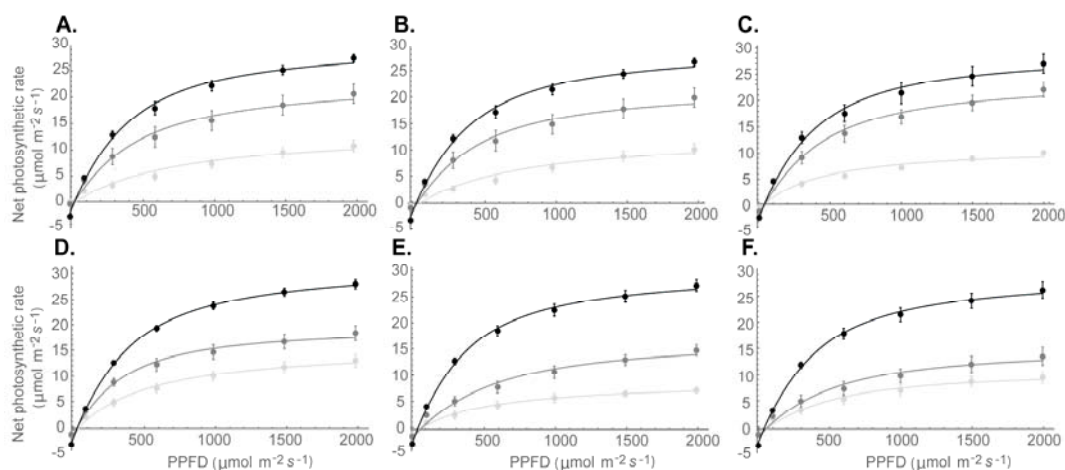


**Figure 4.** Fitted Light response curves for **A-C.** Preanthesis; Parent Line, Line 1 and Line 2, respectively. Layer top (black), middle (dark grey) and bottom (light grey). **D-F.** Postanthesis; Parent Line, Line 1 and Line 2, respectively. Layer top (black), middle (dark grey) and bottom (light grey).

287 there was complete correspondence at the top of the canopy. It is therefore important to  
 288 confirm the activity of specific components of photosynthesis and compare them to both  
 289  $P_{max}$  and  $P_{max}^{opt}$  values. To understand how Rubisco activity might be changing we  
 290 measured ACi responses and performed curve fitting to separate the maximum rate of  
 291 carboxylation ( $V_{cmax}$ ), electron transport ( $J$ ) and end product limitation ( $TPU$ ; see Table  
 292 3).  $V_{cmax}$  values at the top of the canopy are consistent with those observed in other  
 293 studies (e.g. Theobald et al., 1998). As we descend the canopy  $V_{cmax}$  declines  
 294 significantly ( $P < 0.05$ ) in a proportion that is consistent with measured, not modelled,  
 295  $P_{max}$ . Mesophyll conductance ( $G_m$ ) was measured but showed no significant differences  
 296 ( $P < 0.05$ ) between lines or layers.  
 297



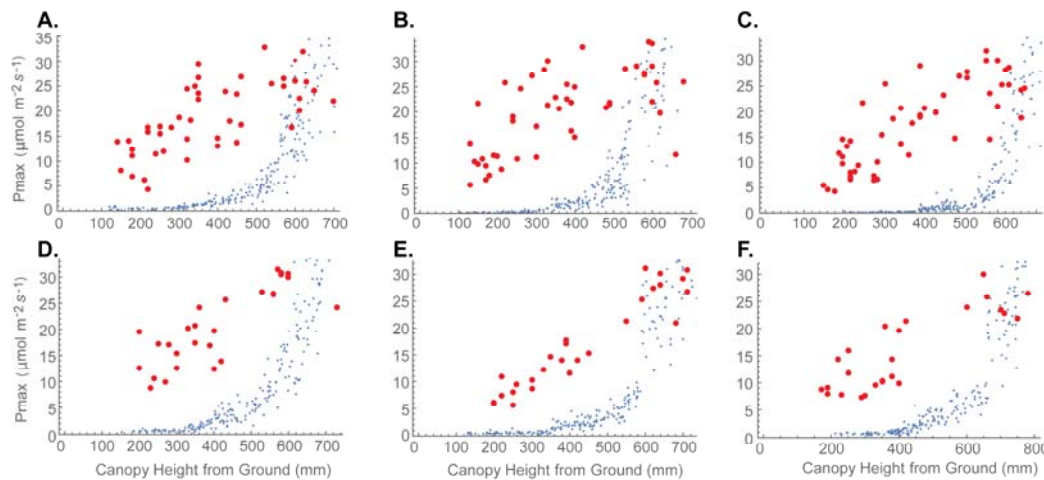


**Figure 5.** Whole canopy acclimation model output (blue) versus gas exchange measurement (red) graphs. The acclimation model was run at 250 locations throughout canopy depth to predict the optimal  $P_{max}$  at each location dependent upon the light environment that it experienced, calculated via ray tracing. The time weighted average (Eq. 4) was fixed at  $\tau=0.2$ . This is an exponentially decaying weight used to represent the fact that photosynthesis is not able to respond instantaneously to a change in irradiance levels. If  $\tau=0$  then a plant will be able to instantaneously respond to a change in irradiance, whereas if  $\tau>0$  the time-weighted average light pattern will relax over the timescale  $\tau$ . Model results are compared to field measured gas exchange. **A-C.** Preanthesis and **D-F.** Postanthesis. **A, D.** Parent Line, **B, E.** Line 1 and **C, F.** Line 2.

298 To analyse photoacclimation further, amounts of Rubisco, total soluble protein (TSP)  
 299 and chlorophyll were quantified (Table 4). Rubisco amounts at the top of the canopy  
 300 were consistent with those towards the upper end for wheat (e.g. Theobald et al., 1998)  
 301 and are highly correlated with measured  $P_{max}$  and  $V_{cmax}$  within the canopy (Fig. 6). This  
 302 indicates that Rubisco content accounts for all values of measured  $P_{max}$  and  $V_{cmax}$ , and  
 303 not the modelled  $P_{max}$  values. Other work using similar techniques to characterise rice  
 304 canopies came to a similar conclusion (Murchie et al., 2002). Chl a:b is a reliable  
 305 indicator of dynamic photoacclimation i.e. fully reversible changes occurring at the  
 306 biochemical level. The changes in Chl a:b are consistent with those expected for  
 307 acclimation of light harvesting complexes (LHC) to a lower light intensity, with the  
 308 lowered ratio indicating a greater investment into peripheral LHCII (Murchie and  
 309 Horton, 1997). Interestingly the largest change in Chl a:b occurs in the upper half of the  
 310 canopy where the greatest proportional change in light level occurs.

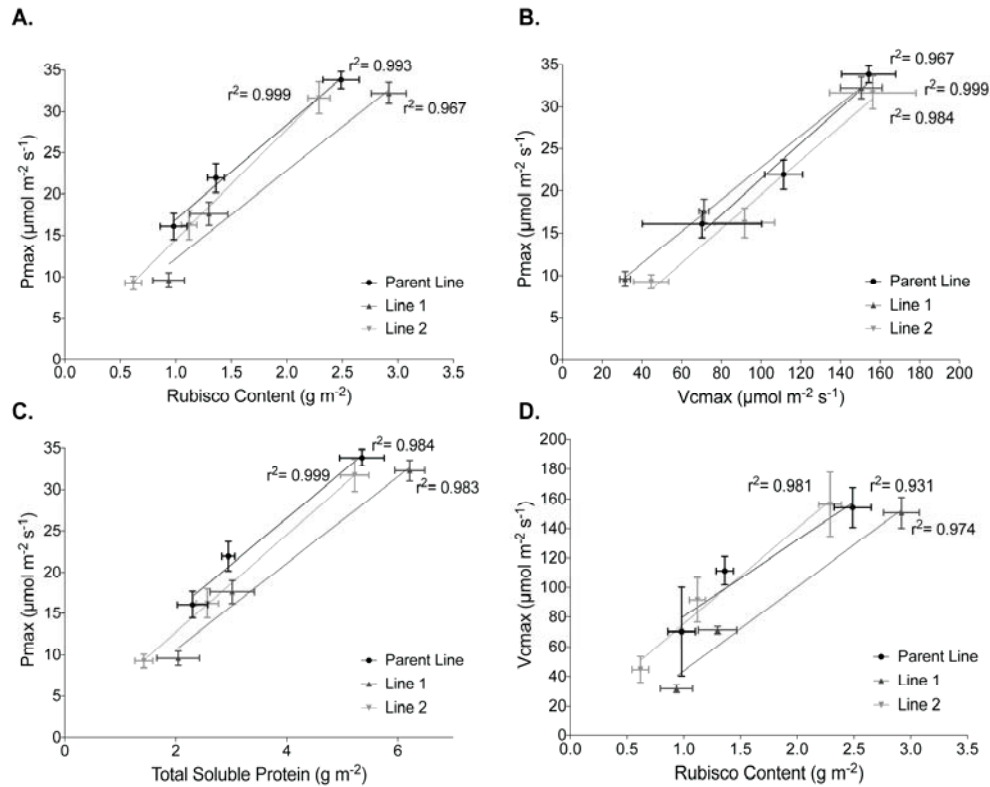


**Figure 6.** Relationships between photosynthesis ( $P_{\max}$  taken from fitted light response curves) and Rubisco properties ( $V_{\text{cmax}}$  from fitted ACi curves and Rubisco/ total soluble protein (TSP) amount) throughout canopy depth, postanthesis; **A.**  $P_{\max}$  and Rubisco content; **B.**  $P_{\max}$  and  $V_{\text{cmax}}$ ; **C.**  $P_{\max}$  and Total Soluble Protein and; **D.**  $V_{\text{cmax}}$  and Rubisco content. Where black (round symbol) in the Parent Line, dark grey (triangle symbol) is Line 1 and light grey (upside down triangle symbol) is Line 2.



## Discussion

The regulatory aspects of photoacclimation and how it is triggered by changing light levels are little understood, but recent work has begun to address this and attempt to elucidate the link between variations in light and the resulting biomass and fitness (e.g. (Külheim *et al.*, 2002; Athanasiou *et al.*, 2010; Retkute *et al.*, 2015; Vialet-Chabrand *et al.*, 2017). In particular, the role of photoacclimation in determining productivity in crop canopies is not known. This paper takes a significant first step and reveals for the first time the relationship between highly realistic canopy architecture, the resulting dynamic light environment and its effect on photoacclimation. In addition to fundamental understanding of photoacclimation, this work has consequences in terms of nutrient usage within our agricultural systems, as discussed below.

Photosynthesis in nature responds largely to fluctuating light, not the unchanging or ‘square waves’ commonly used for studies in photoacclimation (Poorter *et al.*, 2016; Vialet-Chabrand *et al.*, 2017). The responses of leaves within a wheat canopy were analysed to predict the optimal state of photoacclimation using light history as a natural dynamic, rather than fixed or artificially fluctuating, parameter. To do this, a framework of image-based 3D canopy reconstruction and ray tracing combined with mathematical modelling was employed to predict the optimal distribution of photosynthetic acclimation states throughout a field grown wheat canopy based on the realistic dynamic light environment it experiences. The field measured and modelled data indicate two key features: (i) photosynthesis can vary greatly at the same canopy height according to both photoacclimation and instantaneous irradiance shifts and (ii) whilst the model indicates good correspondence to field data at the top of the canopy, the model consistently predicts lower optimal  $P_{max}$  values in the bottom canopy layers relative to measured data. These predictions are important because they consider the effects of fluctuating light in each layer. We conclude that the high light events at the base of the canopy are too short and infrequent to represent a substantial carbon resource for crop biomass. From this we conclude that plants are not optimising leaf composition in response to the long-term light levels they are experiencing, but rather are retaining excessive levels of photosynthetic enzymes at lower canopy levels. As discussed below the latter probably represents an intrinsic influence that could include developmental processes and nutrient remobilisation. Regardless of the cause it also signifies ‘untapped’ photosynthetic potential and opportunities to improve (photosynthetic) nutrient use efficiency.

### 348 ***Influence of Canopy Light Dynamics on Acclimation***

349 Mono-species crop canopies have more consistent structural patterns in comparison  
350 with natural systems, and are useful models for this type of work since data can be  
351 classified according to stratification, but still include spatial complexity and an inherent  
352 stochastic component. Photoacclimation according to canopy level is an expected  
353 property (Supplementary Fig. S1). The dynamic nature of the in-canopy light  
354 environment means that any leaf may be exposed to a range of conditions; from light-  
355 saturation to light limitation, but with varying probability of either according to canopy  
356 depth. Fig. 3 shows clearly how leaves at the top of the canopy experience high  
357 likelihood of direct radiation with fluctuations ranging from two – three-fold depending  
358 on leaf position. Lower in the canopy, occlusion results in an increasing dominance of  
359 diffuse and low levels of radiation punctuated by brief and rare high light events  
360 (sunflecks) that can be 10 – 50 times the mean level. Both the measured and modelled  
361 canopy light levels indicate that the optimal photosynthesis should be low, based upon  
362 the low, basal, levels of light the lower canopy layers receive. This is in agreement with  
363 the modelled  $P_{max}$  values, however, the measured  $P_{max}$  values are much higher than this  
364 (Fig. 5). The key question therefore is whether maintaining higher  $P_{max}$  is beneficial and  
365 necessary to exploit sunflecks?

366

367 Much previous literature has discussed the importance of exploiting sunflecks as a  
368 carbon resource in light-limited environments, such as forest understories (Pearcy,  
369 1990) and the role of fluctuating light in determining photosynthesis – for which  
370 nitrogen profiling in canopies has been discussed (Hikosaka, 2016). However, the  
371 response seems to be variable, depending on physiological acclimation of each species  
372 and stresses associated with increased temperatures and high light (Watling et al., 1997;  
373 Leakey et al., 2005). Here, the use of a novel acclimation model allows us to assess the  
374 effectiveness of photoacclimation in terms of carbon gain at each position in realistic  
375 canopy reconstructions. As sunflecks become rare in the lower portions of the canopy,  
376 the model predicts that acclimation of  $P_{max}$  towards higher values becomes an  
377 increasingly ineffective strategy in terms of exploiting them for carbon gain. To  
378 efficiently exploit the sunflecks in the lower canopy positions, it is necessary to have a  
379 high photosynthetic capacity ( $P_{max}$ ), a rapid rate of photosynthetic induction and a  
380 degree of photoprotective tolerance to avoid photoinhibition. The latter point is not

381 accounted for in this paper but has been noted in other species, especially where much  
382 higher leaf temperatures are involved (Leakey et al., 2005). Photoinhibition (Fv/Fm  
383 lower than 0.8) in lower parts of wheat canopies in the UK was not observed in this  
384 study (data not shown), or in a previous study (Burgess et al., 2015) and in our  
385 temperate system we do not expect excessive leaf temperatures. It is possible that high  
386  $P_{max}$  observed in lower layers of the canopy help to prevent excessive photoinhibition.  
387 Photosynthetic induction state is determined by the previous light history of the leaf; by  
388 stomatal dynamics and the activation state of key enzymes such as Rubisco.  
389 Acclimation of  $P_{max}$  becomes more effective in terms of overall carbon gain where there  
390 is a lower frequency of light transitions but increasing duration of high light events  
391 (Retkute et al., 2015). This is consistent with the light data (Fig. 3), which shows rare,  
392 brief high light events lower in the wheat canopy.

393

394 Such very low levels of light within a crop canopy are comparable with forest floors  
395 where morphological and molecular adaptations are used to enhance light harvesting,  
396 carbon gain and avoid photoinhibition during high light periods (Powles and Bjorkman,  
397 1981; Raven, 1994; Sheue et al., 2015). The interesting feature of cereal canopy  
398 development is the fact that leaves initially develop in high light and then are  
399 progressively shaded as the canopy matures. Since the morphology of the leaf is  
400 determined prior to emergence, all acclimation to low light, post emergence, must be at  
401 the biochemical level, as shown by the chlorophyll a:b ratio (Murchie et al., 2005). The  
402 low light levels within the wheat canopy also require effective acclimation of  
403 respiration rates to maintain positive carbon gain, and this was observed here (Fig. 4).  
404 Leaf respiration is a critical aspect of photoacclimation, permitting lowered light  
405 compensation points and positive carbon balance in low light. The relatively low rates  
406 of dark respiration in the lower layers and the very low measured light levels at the base  
407 of the canopy indicate that leaves maintain their (measured) high  $P_{max}$  alongside low  
408 respiration rates and light compensation points. Therefore, there must be some  
409 decoupling of  $P_{max}$  from these other photoacclimation processes at lower light levels.  
410 The importance of  $R_d$  should be stated here due to its importance in derivation of the  
411 term  $\alpha$  and for confirmation that the same relationship between  $R_d$  and  $\alpha$  holds  
412 regardless of the nature of the fluctuating light environment. However, first  
413 improvements must be made for the accurate measurement of  $R_d$ . This would also allow  
414 for detailed studies on the acclimation of  $R_d$  to a change in light levels.

415

416 We conclude, perhaps surprisingly, that the optimal strategy in lower parts of the  
417 wheat canopy where light is extremely low ( $<50 \mu\text{mol m}^{-2} \text{s}^{-1}$ ) should not be geared  
418 towards exploiting sunflecks (previously seen as an important carbon resource) but  
419 towards light harvesting, maintenance of low leaf respiration and low light  
420 compensation point. Indeed, the photoacclimation of  $P_{max}$  to higher levels requires  
421 substantial investments of resources such as energy, N and C. It is still possible that the  
422 high measured  $P_{max}$  may allow a greater ability to exploit some sunflecks of increased  
423 duration where they do not lead to substantial photoinhibition (Raven, 2011). It is likely  
424 that the planting density has an effect: in this experiment, we have used standard sowing  
425 rates for the UK where the LAI is reasonably high leading to a dense canopy. The  
426 excessive accumulation of Rubisco in lower leaves may be more useful for exploiting  
427 light in planting systems where spacing is greater and light penetration is higher (Parry  
428 et al., 2010). There is little genetic variation for  $P_{max}$ , respiration rate and light  
429 compensation point in the three lines presented here (Fig. 4) although ongoing research  
430 is aimed at identifying further sources of genetic variation for improving these traits  
431 (Parry et al., 2010; Reynolds et al., 2012). Future studies will also need to focus on  
432 enhancing photoacclimation in flag leaf and L2.

433

#### 434 ***Implications in terms of Nutrient Budgeting***

435 The disparity between modelled data and manually measured data has consequences  
436 in terms of the canopy nutrient budget. Photosynthetic components are a significant sink  
437 for leaf N: chloroplasts account for up to 80 % of total leaf N, with Rubisco being the  
438 dominant enzyme (Makino and Osmond, 1991; Evans, 1989; Theobald et al., 1998).  
439 Higher photosynthetic capacity therefore requires a higher N (Evans and Terashima,  
440 1987; Terashima and Evans, 1988; Verhoeven et al., 1997; Evans and Poorter, 2001;  
441 Terashima et al., 2005; Niinemets and Anten, 2009). Photoacclimation to high  
442 irradiance is often associated with an increase in the synthesis of Rubisco per unit leaf  
443 area (Evans and Terashima, 1987) and PNUE will therefore remain high only if the high  
444 irradiance is sustained. The decay of light within plant canopies commonly results in a  
445 correlation between distribution of photosynthetic capacity, light and specific leaf N  
446 (Anten et al., 1995; de Pury and Farquhar 1997; Hikosaka, 2016). However, in ‘real’  
447 canopies the correlation is often not linear, leading to the conclusion that the  
448 relationship is suboptimal, either as an over-accumulation of N in lower regions of the  
449 canopy or an inability to photoacclimate to higher light (Buckley et al., 2013; Hikosaka,

2016). There appears to be species variation within these relationships: a recent meta-analysis showed that the N extinction coefficient for wheat was determined by LAI alone, whereas in other species it was co-determined by the light extinction coefficient (Moreau et al., 2012; Hikosaka, 2016). In the literature many other reasons have been given for this lack of correspondence including herbivory and stomatal and mesophyll limitation (Hikosaka, 2016). The novelty with the current work is the extent of disparity between predicted and optimal  $P_{max}$  at most canopy levels.

Wheat plants and other cereals exhibit a pattern of storage of N in leaves, leaf sheaths and stems prior to grain filling, whereby a substantial proportion of stored N is remobilised toward the grain where it contributes to protein synthesis (Foulkes and Murchie, 2011; Gaju et al., 2011; Moreau et al., 2012). For bread wheat, this is especially important for grain quality. Similar mechanisms occur in many plant species to conserve nutrients, therefore the retention of N in leaves represents a strategy for storage in the latter part of the plant life. Since wheat leaves develop in high light and become progressively shaded, their net lifetime contribution to canopy photosynthesis within the shaded environment will still be substantial. This secondary property of photosynthetic enzymes for N storage has been discussed previously e.g. Sinclair and Sheehy (1999). It is clear that this role is valid, but it is still not certain how it is effectively coordinated with photosynthetic productivity since remobilisation and subsequent senescence represent a compromise to canopy carbon gain in the latter grain filling periods. In this case, it is clear that the accumulation and retention of N in lower leaves of the wheat canopy is dominant over the regulation of key components of optimal photoacclimation, especially  $P_{max}$ , and it is doubtful whether the excess N is used to promote carbon gain at the canopy level. The mechanism for this partitioning ‘strategy’ is not known: it is still possible that the metabolic cost of removing the leaf N is simply greater than the cost of retaining it in the leaves. Were this to be the case then it implies a high degree of precision of the leaf photoacclimation process that is linked to whole plant metabolism. Therefore, questions must be raised as to the cost of this accumulation and whether all N is efficiently remobilised to improve grain quality. Recent data for UK wheat shows that only 76 % of leaf N is remobilised, indicating that a substantial improvement in NUE could be achieved with no penalty for photosynthesis or grain quality (Pask et al., 2012). However, this value is even lower for other plant components, with only 48% of N stored in the stem and 61% stored in the

484 leaf sheath remobilised to the grain (Pask et al., 2012). Altering the photoacclimation  
485 responses of the lower leaves to fluctuating light could bring about this improvement.

486

487 Cross-species correlations between leaf N content and dark respiration have been  
488 observed raising a further question over the respiratory cost of accumulating leaf N in  
489 such low light levels where the opportunities to exploit sunflecks are not high, nor are  
490 warranted in terms of photoacclimation of  $P_{max}$  (Reich et al., 1998). Sinclair and Sheehy  
491 (1999) pointed out that the erect nature of rice leaves had an important effect in terms of  
492 improving the capacity of the lower leaves to store N for remobilisation. Further, we  
493 suggest that even small changes in canopy architecture or physical properties (Burgess  
494 et al., 2015; 2016) would permit lower leaves to operate more efficiently as N storage  
495 organs in addition to their role as net carbon contributors.

496

#### 497 *Concluding remarks*

498 Photosynthetic acclimation permits photosynthesis to optimise to the prevailing light  
499 conditions but its regulation in natural fluctuating light is poorly understood. Here we  
500 show that the accumulation of excessive photosynthetic capacity does not in fact allow  
501 exploitation of sunflecks for enhanced carbon gain, and is not optimal for exploiting the  
502 wheat canopy light environment as revealed by high resolution 3D reconstruction  
503 methods. This observation has some profound implications for the improvement of  
504 canopy photosynthesis and resource use efficiency in crops. First, the unused  
505 photosynthetic potential in lower parts of the canopy (which can be achieved without  
506 the addition of extra nutrients) could be used to enhance biomass and grain yield  
507 through increasing light penetration and reducing the inherent plant-plant competition.  
508 This can be achieved by previously published routes for example architecture (Burgess  
509 et al., 2015), by altering the distribution of chlorophyll content (Zhu et al., 2010; Ort &  
510 Melis, 2011) and/or by manipulating mechanical properties to optimise movement in  
511 response to low wind levels (Burgess et al., 2016). Second, there is an opportunity to  
512 improve photosynthetic nutrient use efficiency: we have shown that levels of canopy  
513 nutrients (especially N) could be reduced with no detrimental impact on either carbon  
514 gain or grain protein content.

## Materials and Methods

### Plant Material

Wheat lines with contrasting canopy architectures were selected from an ongoing field trial at the University of Nottingham farm (Sutton Bonington Campus), Leicestershire UK (52.834 N, 1.243 W) on a sandy loam soil type (Dunnington Heath Series) in 2015. 138 Double haploid (DH) lines were developed jointly by Nottingham and CIMMYT from a cross between the CIMMYT large-ear phenotype spring wheat advanced line LSP2 and UK winter wheat cultivar Rialto, as described in Burgess *et al.* (2015). This approach resulted in the formation of a large number of stable lines with contrasting canopy architecture but with values of light saturated photosynthesis consistent with previous published measurements for field grown wheat in the UK (Driever *et al.*, 2014; Gaju *et al.*, 2016). Two DH lines were then selected and each backcrossed three times with the UK spring wheat cultivar Ashby to produce BC<sub>3</sub> plants. The BC<sub>3</sub> lines were selected phenotypically to contrast for tillering and canopy architecture phenotypes. The BC<sub>3</sub> lines were then selfed for 5 generations before bulking seed of BC<sub>3</sub>S<sub>5</sub> plants for the present trial. Three wheat lines were used for analysis: Ashby (the recurrent parent line), and two BC<sub>3</sub> lines, 32-129 (Line 1) and 23-74 (Line 2). This resulted in lines which were well adapted to the UK environment but which provided contrasts for canopy architecture.

The experiment used a completely randomised block design with three replicates. The plot size was 6.00 x 1.65 m and the sowing date was 20 October 2014. Previous cropping was winter oilseed rape. The field was ploughed and power harrowed and rolled after drilling. Seed rate was adjusted by genotype according to 1,000 grain weight to achieve a target seed rate of 300 seeds m<sup>-2</sup>; rows were 0.13 m apart. 192 kg ha<sup>-1</sup> nitrogen fertilizer as ammonium nitrate was applied in a three-split programme. P and K fertilizers were applied to ensure that these nutrients were not limiting. Plant growth regulator was applied at GS31 to reduce the risk of lodging. Herbicides, fungicides and pesticides were applied as required to minimise effects of weeds, diseases and pests. Two growth stages were analysed: preanthesis and postanthesis (equivalent to GS55-71; Zadoks *et al.*, 1974).

## Plant Physical Measurements

Physical measurements were made on plants in the field (see Table 1 plus Supplementary Table S1). The number of plants and shoots within a 1 m section along the middle of each row were counted and averaged across the three replicate plots. This average value was used to calculate the planting density within the plots and thus used to ensure that the reconstructed canopies were representative of field conditions. Plant dry weight and area (excluding ears) was analysed by separating shoot material into stem and leaf sheath, flag leaf lamina and all other leaf lamina before passing them through a leaf area meter (LI3000C, Licor, Nebraska) for 6 replicate plants (2 per plot; those used for the reconstruction of canopies below). Each component was then dried individually in an oven at 80°C for 48 hours or until no more weight loss was noted. Plants were weighed immediately. Measured Leaf Area Index (leaf area per unit ground area: m<sup>2</sup>; LAI) was calculated as the total area (leaf + stem) divided by the area of ground each plant covered (distance between rows x distance within rows) and averaged across the 6 replicate plants.

## Imaging and Ray Tracing

3D analysis of plants was made according to the protocol of Pound et al. (2014) and further details are given in Burgess et al. (2015). An overview of this process is given in Fig. 1. From the sampled and reconstructed plants, canopies were made *in silico* according to Burgess et al. (2015). Two replicate plants representative of the morphology of each wheat line were taken per plot, giving 6 replicates per line, and reconstructed; at least 4 of these were used to form each the final canopies (Fig. 2). The wheat ears (present postanthesis) were manually removed from the resultant mesh as the reconstructing method is unable to accurately represent their form. Reconstructed canopies were formed by duplicating and randomly rotating the plants in a 3x4 grid, with 13 cm between rows and 5 cm within rows (calculated from field measurements). The LAI of each reconstructed canopy was calculated as the area of mesh inside the ray tracing boundaries divided by the ground area. The LAI of the plots were then compared to the LAI for each of the reconstruction plots; see Table 2. Total light per unit leaf area was predicted using a forward ray-tracing algorithm implemented in fastTracer (fastTracer version 3; PICB, Shanghai, China; Song et al., 2013). Latitude was set at 53 (for Sutton Bonington, UK), atmospheric transmittance 0.5, light reflectance 7.5%, light transmittance 7.5%, day 155 and 185 (4<sup>th</sup> June and 4<sup>th</sup> July: Preanthesis and Postanthesis respectively). FastTracer3 calculates light as direct, diffused and transmitted components



separately; these were combined to give a single irradiance levels for all canopy positions. The diurnal course of light intensities over a whole canopy was recorded in 1 minute intervals. The ray tracing boundaries were positioned within the outside plants to reduce boundary effects. To validate the light interception predicted by ray tracing, fractional interception was calculated at different depths throughout the field grown wheat canopies using a ceptometer (AccuPAR). Light levels at the top, three-quarters, half, quarter and bottom of the plant canopies were taken. Five replicates were taken per plot. This was compared with fractional interception calculated from ray tracing (Supplementary Fig. S1).

### **Gas Exchange and Fluorescence**

Measurements were made on field grown wheat in plots in the same week in which the plants were imaged. For light response curves (LRC) and ACi response curves of photosynthesis, leaves were not dark-adapted. Leaf gas exchange measurements (LRC and ACi) were taken with a LI-COR 6400XT infra-red gas-exchange analyser (LI-COR, Nebraska). The block temperature was maintained at 20°C using a flow rate of 500 ml min<sup>-1</sup>. Ambient field humidity was used. LRCs were measured over a series of 7 photosynthetically active radiation (PAR) values between 0 and 2000  $\mu\text{mol m}^{-2} \text{s}^{-1}$ , with a minimum of 2 minutes and a maximum of 3 minutes at each light level moving from low to high. LRCs were measured at 3 different canopy heights; labelled top (flag leaf), middle and bottom, with height above ground being noted. Three replicates were taken per treatment plot per layer, thus leading to 9 replicates per line. Saturation of photosynthesis was verified for each light response step by conducting a separate set of light response curves where photosynthesis was logged every few seconds. It was verified that this protocol resulted in saturation at each light level. For the ACi curves, leaves were exposed to 1500  $\mu\text{mol m}^{-2} \text{sec}^{-1}$ . They were placed in the chamber at 400 p.p.m. CO<sub>2</sub> for a maximum of 2 min and then CO<sub>2</sub> was reduced stepwise to 40 p.p.m. CO<sub>2</sub> was then increased to 1500 p.p.m., again in a stepwise manner. At least one replicate was taken per treatment plot per layer but with 5 replicates taken for each of the 3 lines. Individual ACi curves were fitted using the tool in Sharkey et al. (2007) with leaf temperature set at 20 °C, atmospheric pressure at 101 kPa, O<sub>2</sub> pressure at 21 kPa and limiting factors assigned as suggested in Sharkey et al. (2007). A Walz (Effeltrich, Germany) MiniPam fluorometer was used to measure dark-adapted values of Fv/Fm in the field wheat every hour between 09:00 and 17:00 h. 20 minutes dark adaptation was applied using the

method of Burgess et al. (2015). Four replicates were taken per plot per layer. Measurements were not taken for the bottom layer.

### **Rubisco quantification**

Leaf samples were taken from the same leaves and same region of the leaf as the gas exchange measurements. One day was left between gas exchange and sampling. Leaf samples (1.26 cm<sup>2</sup>) were ground at 4°C in an ice-cold pestle and mortar containing 0.5 mL of 50 mM Bicine-NaOH pH 8.2, 20 mM MgCl<sub>2</sub>, 1 mM EDTA, 2 mM benzamidine, 5 mM ε-aminocaproic acid, 50 mM 2-mercaptoethanol, 10 mM DTT, 1mM PMSF and 1% (v/v) protease inhibitor cocktail (Sigma-Aldrich Co., St Louis, MO, USA). The homogenate was clarified by centrifugation at 14700g and 4°C for 3 min. Rubisco in 150 µL of the supernatant was quantified by the [<sup>14</sup>C]-CABP binding assay (Parry et al., 1997), as described previously (Carmo-Silva et al. 2010). The radioactivity due to [<sup>14</sup>C]-CABP bound to Rubisco catalytic sites was measured by liquid scintillation counting (PerkinElmer, Waltham, MA, USA). Total soluble protein content in the supernatants was determined by the method of Bradford (1976) using bovine serum albumin as a standard. Chlorophylls in 20 µL of the homogenate (prior to centrifugation) were extracted in 95% ethanol for 4-8 hours in darkness (Lichtenthaler, 1987). After clarifying the ethanol-extracted samples by centrifugation at 14000g for 3 min, the absorbance of chlorophylls in ethanol was measured at 649 and 665 nm. Chlorophyll *a* and *b* contents were estimated using the formulas  $C_a = (13.36 \cdot A_{664}) - (5.19 \cdot A_{649})$  and  $C_b = (27.43 \cdot A_{649}) - (8.12 \cdot A_{664})$ .

### **Modelling**

All modelling was carried out using Mathematica (Wolfram) using the techniques described in more detail in Retkute et al., (2015) and Burgess et al., (2015). The acclimation model, here adopted for use in the canopy setting, was originally developed based on the observation that *Arabidopsis thaliana* plants subject to a fluctuating light pattern exhibit a higher  $P_{max}$  than plants grown under a constant light pattern of the same average irradiance (Yin and Johnson, 2000; Athanasiou et al., 2010). The main model assumption is that plants will adjust  $P_{max}$  from a range of possible values in such a way as to produce the largest amount of daily carbon gain. The model predicts an optimal maximum photosynthetic capacity,  $P_{max}^{opt}$ , for a given light pattern from light response curve parameters ( $\phi$ ,  $\theta$  and  $\alpha$ ; explained below).

In this study, we sought to predict the maximum photosynthetic capacity,  $P_{max}^{opt}$ , as the  $P_{max}$  that represents maximal carbon gain at a single point within the canopy, based on the light pattern that point has experienced (i.e. using the light pattern output from ray tracing; as in right hand panel, Fig. 3). This was predicted across 250 canopy points, thus leading to distribution of  $P_{max}^{opt}$  values throughout each of the canopies. These 250 canopy positions (triangles) from each of the canopies were chosen as a subset of triangles that were of similar size (i.e. area) and constitute a representative sample distribution throughout canopy depth.

The net photosynthetic rate,  $P$ , as a function of PPFD,  $L$ , and maximum photosynthetic capacity,  $P_{max}$ , was calculated using the non-rectangular hyperbola (Eq. 1).

$$F_{NRH}(L, \phi, \theta, P_{max}, \alpha) = \frac{\phi L + (1 + \alpha)P_{max} - \sqrt{(\phi L + (1 + \alpha)P_{max})^2 - 4\theta\phi L(1 + \alpha)P_{max}}}{2\theta} - \alpha P_{max} \quad (1)$$

Where  $L$  is the PPFD incident on a leaf ( $\mu\text{mol m}^{-2} \text{s}^{-1}$ ),  $\phi$  is the quantum use efficiency,  $\theta$  is the convexity and  $\alpha$  corresponds to the fraction of maximum photosynthetic capacity ( $P_{max}$ ) used for dark respiration according to the relationship  $Rd = \alpha P_{max}$  (Givnish, 1988; Niinemets and Tenhunen, 1997; Retkute et al., 2015). The value of  $\alpha$  was obtained from the light response curves recorded in the field by fitting a line of best fit between measured  $P_{max}$  and  $R_d$  values for all individual plants ( $n > 20$  plants for each wheat line and stage). Therefore, the relationship between  $P_{max}$  and  $R_d$  used in modelling is based on observation rather than assumption of linear fit. All other parameters (e.g.  $P_{max}$ ,  $\phi$  and  $\theta$ ) were estimated from the light response curves for three canopy layers using the Mathematica command **FindFit**.

As each canopy was divided into 3 layers, each triangle from the digital plant reconstruction was assigned to a particular layer,  $m$ , according to the triangle centre (i.e. with triangle centre between upper and lower limit of a layer depth). For each depth ( $d$ ; distance from the highest point of the canopy), we found all triangles with centres lying above  $d$  (Eq. 2).

$$d_i = \max_{j=1,2,3; 1 \leq i \leq n} z_i^j - (z_i^1 + z_i^2 + z_i^3)/3 \quad (2)$$

Each triangle within a specific layer was assigned the light response curve parameters from the corresponding measured data.

Carbon gain,  $C$  ( $\text{mol m}^{-2}$ ) was calculated over the time period  $t \in [0, T]$  (Eq. 3).

$$C(L(t), P_{max}) = \int_0^T P(L(t), P_{max}) dt \quad (3)$$

Experimental data indicates that the response of photosynthesis to a change in irradiance is not instantaneous and thus to incorporate this into the model Retkute et al. (2015) introduced a time-weighted average for light (Eq. 4).

$$L_\tau(t) = \frac{1}{\tau} \int_{-\infty}^T L(t') e^{-\frac{t-t'}{\tau}} dt' \quad (4)$$

This effectively accounts for photosynthetic induction state, which is very hard to quantify *in situ* as it varies according to the light history of the leaf. The more time recently spent in high light, the faster the induction response. The time-weighted average effectively acts as a “fading memory” of the recent light pattern and uses an exponentially decaying weight. If  $\tau=0$  then a plant will be able to instantaneously respond to a change in irradiance, whereas if  $\tau>0$  the time-weighted average light pattern will relax over the timescale  $\tau$ . Within this study,  $\tau$  was fixed at 0.2 (unless otherwise stated) in agreement with previous studies and fit with past experimental data (Pearcy and Seemann 1990, Retkute et al., 2015). The time-weighted average only applies to the transition from low to high light. From the high to low, response is here considered to be virtually instantaneous and the time-weighted average is not applied. The effect of this decaying weight effectively acts as a “filter” for irradiance levels, with photosynthesis as slow to respond from a transition from low to high light but quick to respond following a drop in irradiance. This can be seen in Supplementary Fig. S3. The value of  $\tau$  (0.2) selected here represents a maximum leaf ‘memory’ of around 12 minutes that exponentially declines according to time spent in the light. We verified this experimentally using wheat leaves grown under irradiance levels that correspond to mid to upper canopy level: induction from darkness to  $1000 \mu\text{mol m}^{-2} \text{s}^{-1}$  typically took 10 – 20 minutes to reach steady state rate. We also tested the model at a lower value of  $\tau$  (0.1) to account for leaves capable of faster induction or a longer ‘memory’ (Supplementary Fig. S4).

## Tables

**Table 1**

Physical canopy measurements of each Genotype. The number of plants and tillers within a 1 m section along a row at the preanthesis stage were counted and averaged across 3 plots. The number of shoots for each of the plants used for reconstructions at preanthesis was counted. The resting plant height of 5 plants per plot was calculated. P value corresponds to ANOVA. Mean  $\pm$  SEM,  $n=3$ .

Line	Average Number of Plants m <sup>-1</sup>	Average Number of Shoots m <sup>-1</sup>	Number of Shoots plant <sup>-1</sup>	Average Resting Plant height (cm)	
				Preanthesis	Postanthesis
Parent	25.3 $\pm$ 1.5	69.0 $\pm$ 3.1	4.0 $\pm$ 0.0	72.1 $\pm$ 3.2	84.7 $\pm$ 0.3
Line 1	21.3 $\pm$ 3.2	61.0 $\pm$ 2.3	3.5 $\pm$ 0.3	68.3 $\pm$ 2.0	90.7 $\pm$ 1.6
Line 2	20.7 $\pm$ 0.3	62.7 $\pm$ 2.7	4.1 $\pm$ 0.9	69.5 $\pm$ 2.7	94.1 $\pm$ 5.5
P value	0.287	0.170	0.675	0.579	0.063

713 **Table 2**

714 Plant and canopy area properties. Plants were separated into leaf and stem material and measured using a leaf area meter (LI3000C, Licor,  
 715 Nebraska). Measured LAI was calculated as the total area (leaf + stem) divided by the area of ground each plant covered (distance between rows  
 716 x distance within rows). The reconstructed LAI was calculated as mesh area inside the designated ray tracing boundaries (see Materials and  
 17 Methods: Imaging and Ray Tracing). P value corresponds to ANOVA. Mean  $\pm$  SEM,  $n=3$

Line	Measured (plant <sup>-1</sup> )			Reconstruction	
	Leaf Area	Stem Area	Total Area	LAI	LAI
Parent	318 $\pm$ 20	93 $\pm$ 4	799 $\pm$ 73	7.22 $\pm$ 1.23	8.55
Line 1	312 $\pm$ 27	66 $\pm$ 10	807 $\pm$ 42	6.71 $\pm$ 1.30	8.39
Line 2	411 $\pm$ 70	82 $\pm$ 10	1118 $\pm$ 113	8.78 $\pm$ 1.90	9.75
P value	0.290	0.167	0.520	0.520	

718 **Table 3**

719 Parameters taken from curve fitting.  $P_{max}$  taken from light response curves and  $V_{cmax}$ ,  $J$ ,  $TPU$ ,  $R_d$  and  $G_m$  taken from ACi curves (fitting at 25°C;  
720 I= 3.74 using Sharkey et al., 2007). Mean  $\pm$  SEM,  $n=9$  for  $P_{max}$  and  $n=5$  for ACi parameters. P value corresponds to ANOVA.

	Line	Layer	$P_{max}$ ( $\mu\text{mol m}^{-2} \text{s}^{-1}$ )	$V_{cmax}$ ( $\mu\text{mol m}^{-2} \text{s}^{-1}$ )	$J$ ( $\mu\text{mol m}^{-2} \text{s}^{-1}$ )	$TPU$ ( $\mu\text{mol m}^{-2} \text{s}^{-1}$ )	$R_d$ ( $\mu\text{mol m}^{-2} \text{s}^{-1}$ )	$G_m$ ( $\mu\text{mol m}^{-2} \text{s}^{-1} \text{Pa}^{-1}$ )
Preanthesis	Parent	Top	30.1±2.2	225±14	305±5	24.0±0.4	5.1±0.5	12.3±7.5
		Middle	25.0±2.0	124±8	232±17	18.2±1.3	3.9±0.7	35.2±7.0
		Bottom	15.6±0.8	80±8	169±16	13.5±1.1	2.1±0.4	37.1±5.1
	Line 1	Top	32.3±0.7	185±19	313±24	24.2±1.9	5.4±1.1	28.1±8.2
		Middle	23.6±1.8	150±37	259±34	19.9±2.9	4.7±1.3	35.0±7.1
		Bottom	12.3±1.4	64±24	103±14	8.3±1.1	3.2±1.1	24.9±10.3
	Line 2	Top	30.3±2.5	200±46	290±24	23.1±2.5	4.2±2.2	37.3±4.9
		Middle	25.8±2.1	111±14	246±25	19.0±1.7	3.3±0.8	34.4±7.8
		Bottom	11.0±0.7	73±13	125±15	10.1±1.2	2.3±0.4	26.1±9.9
	P between Lines		0.638	0.733	0.718	0.691	0.380	0.772
	Mean	Top	30.9	203	303	23.7	4.90	25.9
		Middle	24.8	128	246	19.0	3.96	35.0
		Bottom	13.0	73	134	10.8	2.52	29.7
	P between layers		<0.001	<0.001	<0.001	<0.001	0.042	0.351
Postanthesis	Parent	Top	33.8±1.0	154±14	251±25	19.3±2.0	4.1±0.8	12.3±7.5
		Middle	21.9±1.8	111±10	207±20	16.1±1.6	2.7±0.3	26.9±8.7
		Bottom	16.1±1.6	70±30	106±19	8.6±1.4	1.8±0.5	26.5±9.6
	Line 1	Top	32.3±1.3	150±11	253±16	19.8±1.2	2.5±0.5	14.0±7.2
		Middle	17.6±1.4	71±2	132±6	10.3±0.5	1.2±0.2	36.0±6.2



Line 2	Bottom	9.6±0.9	31±3	65±7	5.4±0.4	1.3±0.2	28.0±8.6
	Top	31.7±1.9	156±22	262±15	20.7±0.9	4.1±0.7	17.8±7.3
	Middle	16.2±1.8	92±15	187±23	14.6±1.7	2.4±0.6	36.7±5.5
	Bottom	9.3±0.8	45±9	90±8	7.5±0.5	1.7±0.3	42.2±0.2
P between Lines		<0.001	0.106	0.027	0.024	0.012	0.009
Mean	Top	32.6	154	255	20.0	3.58	14.7
	Middle	18.5	92	175	13.7	2.08	33.2
	Bottom	11.7	50	87	7.1	1.60	30.7
P between Layers		<0.001	<0.001	<0.001	<0.001	<0.001	0.330

732 **Table 4**

733 Rubisco, total soluble protein and chlorophyll content plus chlorophyll a:b and Rubisco: chlorophyll ratios with each layer through the canopy at  
734 the postanthesis stage. Means  $\pm$  SEM,  $n=6$ . P value corresponds to ANOVA.

Line	Layer	Rubisco (g m <sup>-2</sup> )	TSP (g m <sup>-2</sup> )	Chlorophyll (mg m <sup>-2</sup> )	Chlorophyll a:b	Rubisco : Chlorophyll
Parent	Top	2.49 $\pm$ 0.16	5.35 $\pm$ 0.40	844 $\pm$ 49	1.93 $\pm$ 0.04	2.95 $\pm$ 0.11
	Middle	1.36 $\pm$ 0.08	2.95 $\pm$ 0.12	723 $\pm$ 21	1.79 $\pm$ 0.03	1.88 $\pm$ 0.09
	Bottom	0.98 $\pm$ 0.12	2.30 $\pm$ 0.27	602 $\pm$ 46	1.79 $\pm$ 0.02	1.61 $\pm$ 0.01
Line 1	Top	2.92 $\pm$ 0.16	6.22 $\pm$ 0.27	820 $\pm$ 28	1.98 $\pm$ 0.05	3.58 $\pm$ 0.23
	Middle	1.30 $\pm$ 0.17	3.02 $\pm$ 0.40	667 $\pm$ 39	1.79 $\pm$ 0.02	1.92 $\pm$ 0.15
	Bottom	0.94 $\pm$ 0.14	2.04 $\pm$ 0.38	532 $\pm$ 55	1.68 $\pm$ 0.03	1.74 $\pm$ 0.16
Line 2	Top	2.29 $\pm$ 0.10	5.22 $\pm$ 0.26	734 $\pm$ 36	1.99 $\pm$ 0.04	3.13 $\pm$ 0.10
	Middle	1.12 $\pm$ 0.07	2.57 $\pm$ 0.20	618 $\pm$ 20	1.75 $\pm$ 0.03	1.81 $\pm$ 0.07
	Bottom	0.62 $\pm$ 0.07	1.43 $\pm$ 0.16	440 $\pm$ 51	1.72 $\pm$ 0.05	1.41 $\pm$ 0.07
P between Lines		0.002	0.019	0.002	0.763	0.015
Mean	Top	2.57	5.60	799	1.96	3.22
	Middle	1.26	2.85	669	1.78	1.87
	Bottom	0.85	1.93	525	1.73	1.58
P between Layers		<0.001	<0.001	<0.001	<0.001	<0.001

## 735 **Figure Legends**

736 **Figure 1:** Overview of the reconstruction process A. original photograph, B. point  
737 cloud reconstruction using stereocameras (Wu, 2011), C. output point cloud, D. mesh  
738 following reconstruction method (Pound et al., 2014) and E. final canopy  
739 reconstruction. N.B. The multi-coloured disc in panels a-c is a calibration target, used to  
740 optimise the reconstruction process and scale the final reconstructions back to their  
741 original units.

742

743 **Figure 2:** Example Canopy Reconstructions from front and top down views. A-C.  
744 Preanthesis and D-F. Postanthesis. A, D. Parent Line, B, E. Line 1 and C, F. Line 2

745

746 **Figure 3:** Progressive lowering of the canopy position in a canopy results in a reduction  
747 in daily integrated PPFD ( $\mu\text{mol m}^{-2} \text{s}^{-1}$ ) but also the pattern and incidence of high light  
748 events within the canopy. The left hand panel shows a representative reconstructed  
749 preanthesis wheat canopy with a single plant in bold: Maximum PPFD ranges are  
750 colour coded. The right hand panels show PPFD during the course of a day at 9  
751 representative and progressively lower canopy positions (the height of each canopy  
752 location from the ground given in the top left corner of each graph) calculated using ray  
753 tracing techniques.

754

755 **Figure 4:** Fitted Light response curves for A-C. Preanthesis; Parent Line, Line 1 and  
756 Line 2, respectively. Layer top (black), middle (dark grey) and bottom (light grey). D-F.  
757 Postanthesis; Parent Line, Line 1 and Line 2, respectively. Layer top (black), middle  
758 (dark grey) and bottom (light grey).

759

760 **Figure 5:** Whole canopy acclimation model output (blue) versus gas exchange  
 761 measurement (red) graphs. The acclimation model was run at 250 locations throughout  
 762 canopy depth to predict the optimal  $P_{max}$  at each location dependent upon the light  
 763 environment that it experienced, calculated via ray tracing. The time weighted average  
 764 (Eq. 4) was fixed at  $\tau=0.2$ . This is an exponentially decaying weight used to represent  
 765 the fact that photosynthesis is not able to respond instantaneously to a change in  
 766 irradiance levels. If  $\tau=0$  then a plant will be able to instantaneously respond to a change in  
 767 irradiance, whereas if  $\tau>0$  the time-weighted average light pattern will relax over the  
 768 timescale  $\tau$ . Model results are compared to field measured gas exchange. A-C.  
 769 Preanthesis and D-F. Postanthesis. A, D. Parent Line, B, E. Line 1 and C, F. Line 2.  
 770

771 **Figure 6:** Relationships between photosynthesis ( $P_{max}$  taken from fitted light response  
 772 curves) and Rubisco properties ( $V_{cmax}$  from fitted ACi curves and Rubisco/ total soluble  
 773 protein (TSP) amount) throughout canopy depth; A.  $P_{max}$  and Rubisco content; B.  $P_{max}$   
 774 and  $V_{cmax}$ ; C.  $P_{max}$  and Total Soluble Protein and; D.  $V_{cmax}$  and Rubisco content. Where  
 775 black (round symbol) in the Parent Line, dark grey (triangle symbol) is Line 1 and light  
 776 grey (upside down triangle symbol) is Line 2.

777 **Supplementary Data**

778 **Supplementary Table S1**

779 Plant physiological measurements (plant height and leaf dimensions), preanthesis. Mean  
780  $\pm$  SEM, n=3.

781 **Supplementary Figure S1:** Experimental validation of the predicted light levels.

782 **Supplementary Figure S2:** Example of a time-weighted light pattern at  $\tau=0.2$  relative  
783 to a non-weighted line.

784 **Supplementary Figure S3:** Model output (blue) versus gas exchange measurement  
785 (red) graphs for the Parent Line, preanthesis.

786 **Supplementary Figure S4:** Whole canopy acclimation model output (blue) versus gas  
787 exchange measurement (red) graphs.

788

789

790 **Supplementary Table S1**

791 Plant physiological measurements (plant height and leaf dimensions), preanthesis. Mean  
792  $\pm$  SEM, n=3.

793

794 **Supplementary Figure S1:** Experimental validation of the predicted light levels. The  
795 logarithm of the ratio of the light received on a horizontal surface and light intercepted  
796 on a point on a leaf ( $\ln[L/L_0]$ ) predicted by ray tracing (box and whisker) is compared  
797 to manual measurements made using a ceptometer (stars). Predicted and measured data  
798 for A. Parent Line, B. Line 1 and C. Line 2; top, middle and bottom layers of the  
799 canopy at 12:00 h.

800

801 **Supplementary Figure S2:** Example of a time-weighted light pattern at  $\tau=0.2$  (black  
802 line) relative to a non-weighted line (i.e.  $\tau=0$ ). Light patterns for A. top, B. middle and  
803 C. bottom canopy layers (as shown in Fig. 3). The time weighted average (Eq. 4) is an  
804 exponentially decaying weight used to represent the fact that photosynthesis is not able  
805 to respond instantaneously to a change in irradiance levels. If  $\tau=0$  then a plant will be able  
806 to instantaneously respond to a change in irradiance, whereas if  $\tau>0$  the time-weighted  
807 average light pattern will relax over the timescale  $\tau$ . Within this study,  $\tau$  was fixed at 0.2  
808 unless otherwise stated.

809

810 **Supplementary Figure S3:** Model output (blue) versus gas exchange measurement  
811 (red) graphs for the Parent Line, preanthesis. A.  $P_{max}$  against the PPFD at 12:00 h.

812 Modelled PPFD is taken from the ray tracing output whereas measured PPFD is taken  
813 from ceptometer data in the field; N.B. ceptometer measurements were taken at a  
814 quarter, half and three quarters up the canopy, relating to bottom, middle and top layers,  
815 respectively, so the data was grouped accordingly. B. modelled daily integrated PPFD  
816 versus modelled  $P_{max}$ .

817

818 **Supplementary Figure S4:** Whole canopy acclimation model output (blue) versus gas  
819 exchange measurement (red) graphs. The acclimation model was run at 250 locations  
820 throughout canopy depth to predict the optimal  $P_{max}$  at each location dependent upon the  
821 light environment that it experienced, calculated via ray tracing. The time weighted  
822 average (Eq. 4) was fixed at  $\tau=0.1$ . This is an exponentially decaying weight used to  
823 represent the fact that photosynthesis is not able to respond instantaneously to a change  
824 in irradiance levels. If  $\tau=0$  then a plant will be able to instantaneously respond to a change  
825 in irradiance, whereas if  $\tau>0$  the time-weighted average light pattern will relax over the  
826 timescale  $\tau$ . Results shown for the Parent Line, Preanthesis.

827

828 **Acknowledgements**

829 We thank Prof Xinguang Zhu and Dr Qinfeng Song (Shanghai Institute for Biological  
830 Sciences) for useful input concerning the ray tracer and the following for useful  
831 discussions: Prof Martin Parry (Lancaster University), Dr Mike Pound (University of  
832 Nottingham), Prof Tony Pridmore (University of Nottingham), Dr Simon Preston  
833 (University of Nottingham), Dr Ian Smillie (Licor Inc., Cambridge, UK) and Prof  
834 Oliver Jensen (University of Manchester). We thank Dr Peter Werner (KWS UK Ltd)  
835 for developing the BC<sub>3</sub> lines.

836

837



## Parsed Citations

**Anderson, J.M., Chow, W.S. and Park, Y.I. (1995)** The grand design of photosynthesis: acclimation of the photosynthetic apparatus to environmental cues. *Photosynthesis Research*, 46, 129–139.

Pubmed: [Author and Title](#)  
CrossRef: [Author and Title](#)  
Google Scholar: [Author Only](#) [Title Only](#) [Author and Title](#)

**Anderson, J.M. and Osmund, C.B. (1987)** Shade-Sun responses: compromises between acclimation and photoinhibition. In: Kyle, D.J., Osmond, C.B. and Arntzen, C.J. (eds.) *Photoinhibition*. Amsterdam: Elsevier Science bv. Amsterdam, Netherlands, pp. 1–38.

Pubmed: [Author and Title](#)  
CrossRef: [Author and Title](#)  
Google Scholar: [Author Only](#) [Title Only](#) [Author and Title](#)

**Anten, N.P., Schieving, F. and Werger, M.J. (1995)** Patterns of light and nitrogen distribution in relation to whole canopy carbon gain in C3 and C4 mono- and dicotyledonous species. *Oecologia*, 101, 504–513.

Pubmed: [Author and Title](#)  
CrossRef: [Author and Title](#)  
Google Scholar: [Author Only](#) [Title Only](#) [Author and Title](#)

**Athanasίου, K., Dyson, B.C., Webster, R.E. and Johnson, G.N. (2010)** Dynamic acclimation of photosynthesis increases plant fitness in changing environments. *Plant Physiology*, 152, 366–373.

Pubmed: [Author and Title](#)  
CrossRef: [Author and Title](#)  
Google Scholar: [Author Only](#) [Title Only](#) [Author and Title](#)

**Björkman, O. (1981)** Responses to different quantum flux densities. In: Lange, O.L., Nobel, P.S., Osmond, C.B. and Ziegler, H. (eds.) *Physiological Plant Ecology*, Springer, pp. 57–107.

Pubmed: [Author and Title](#)  
CrossRef: [Author and Title](#)  
Google Scholar: [Author Only](#) [Title Only](#) [Author and Title](#)

**Bradford, M.M. (1976)** A rapid and sensitive method for the quantitation of microgram quantities of protein utilizing the principle of protein-dye binding. *Analytical Biochemistry*, 72, 248–254.

Pubmed: [Author and Title](#)  
CrossRef: [Author and Title](#)  
Google Scholar: [Author Only](#) [Title Only](#) [Author and Title](#)

**Buckley, T.N., Cescatti, A. and Farquhar, G.D. (2013)** What does optimization theory actually predict about crown profiles of photosynthetic capacity when models incorporate greater realism? *Plant, Cell and Environment*, 36, 1547–1563.

Pubmed: [Author and Title](#)  
CrossRef: [Author and Title](#)  
Google Scholar: [Author Only](#) [Title Only](#) [Author and Title](#)

**Burgess, A.J., Retkute, R., Pound, M.P., Preston, S.P., Pridmore, T.P., Foulkes, M.J., Jensen, O.E. and Murchie, E.H. (2015)** High-resolution 3D structural data quantifies the impact of photoinhibition on long term carbon gain in wheat canopies in the field. *Plant Physiology*, 169, 1192–1204.

Pubmed: [Author and Title](#)  
CrossRef: [Author and Title](#)  
Google Scholar: [Author Only](#) [Title Only](#) [Author and Title](#)

**Burgess, A.J., Retkute, R., Preston, S.P., Jensen, O.E., Pound, M.P., Pridmore, T.P. and Murchie, E.H. (2016)** The 4-dimensional plant: effects of wind-induced canopy movement on light fluctuations and photosynthesis. *Frontiers in Plant Science*, 7, 1392.

Pubmed: [Author and Title](#)  
CrossRef: [Author and Title](#)  
Google Scholar: [Author Only](#) [Title Only](#) [Author and Title](#)

**Carmo-Silva, A.E., Keys, A.J., Andralojc, P.J., Powers, S.J., Arrabaça, M.C. and Parry, M.A.J. (2010)** Rubisco activities, properties, and regulation in three different C4 grasses under drought. *Journal of Experimental Botany*, 61, 2355–2366.

Pubmed: [Author and Title](#)  
CrossRef: [Author and Title](#)  
Google Scholar: [Author Only](#) [Title Only](#) [Author and Title](#)

**Carmo-Silva, A.E. and Salvucci, M.E. (2013)** The regulatory properties of Rubisco activase differ among species and affect photosynthetic induction during light transitions. *Plant Physiology*, 161, 1645–1655.

Pubmed: [Author and Title](#)  
CrossRef: [Author and Title](#)  
Google Scholar: [Author Only](#) [Title Only](#) [Author and Title](#)

**Chabot, B.F., Jurik, T.W. and Chabot, J.F. (1979)** Influence of instantaneous and integrated light-flux density on leaf anatomy and photosynthesis. *American Journal of Botany*, 66, 940–945.

Pubmed: [Author and Title](#)  
CrossRef: [Author and Title](#)  
Google Scholar: [Author Only](#) [Title Only](#) [Author and Title](#)

de Pury, D.G.G. and Farquhar, G.D. (1997) Simple scaling of photosynthesis from leaves to canopies without the errors of big-leaf models. *Plant, Cell and Environment*, 20(5), 537–557.

Pubmed: [Author and Title](#)

CrossRef: [Author and Title](#)

Google Scholar: [Author Only Title Only Author and Title](#)

Driever, S., Lawson, T., Andralojc, P., Raines, C. and Parry, M.A. (2014) Natural variation in photosynthetic capacity, growth, and yield in 64 field-grown wheat genotypes. *Journal of Experimental Botany*, 65, 4959–4973.

Pubmed: [Author and Title](#)

CrossRef: [Author and Title](#)

Google Scholar: [Author Only Title Only Author and Title](#)

Evans, J.R. (1989) Photosynthesis and nitrogen relationships in leaves of C3 plants. *Oecologia*, 78, 9–19.

Pubmed: [Author and Title](#)

CrossRef: [Author and Title](#)

Google Scholar: [Author Only Title Only Author and Title](#)

Evans, J.R. and Poorter, H. (2001) Photosynthetic acclimation of plants to growth irradiance: the relative importance of specific leaf area and nitrogen partitioning in maximizing carbon gain. *Plant, Cell and Environment*, 24, 755–767.

Pubmed: [Author and Title](#)

CrossRef: [Author and Title](#)

Google Scholar: [Author Only Title Only Author and Title](#)

Evans, J.R. and Terashima, I. (1987) Effects of nitrogen nutrition on electron transport components and photosynthesis in spinach. *Functional Plant Biology*, 14, 59–68.

Pubmed: [Author and Title](#)

CrossRef: [Author and Title](#)

Google Scholar: [Author Only Title Only Author and Title](#)

Foulkes, M.J. and Murchie, E.H. (2011) Optimizing canopy physiology traits to improve the nutrient use efficiency of crops. In: Hawkesford, M.J. & Barraclough, P. (eds.) *The Molecular and physiological basis of nutrient use efficiency in crops*. Chichester, Wiley-Blackwell, pp. 65–83.

Pubmed: [Author and Title](#)

CrossRef: [Author and Title](#)

Google Scholar: [Author Only Title Only Author and Title](#)

Gaju, O., Allard, V., Martre, P., Snape, J.W., Heumez, E., LeGouis, J., Moreau, D., Bogard, M., Griffiths, S., Orford, S. and Hubbart, S. (2011) Identification of traits to improve the nitrogen-use efficiency of wheat genotypes. *Field Crops Research*, 123(2), 139–152.

Pubmed: [Author and Title](#)

CrossRef: [Author and Title](#)

Google Scholar: [Author Only Title Only Author and Title](#)

Gaju, O., DeSilva, J., Carvalho, P., Hawkesford, M.J., Griffiths, S., Greenland, A. and Foulkes, M.J. (2016) Leaf photosynthesis and associations with grain yield, biomass and nitrogen-use efficiency in landraces, synthetic-derived lines and cultivars in wheat. *Field Crops Research*, 193, 1–15.

Pubmed: [Author and Title](#)

CrossRef: [Author and Title](#)

Google Scholar: [Author Only Title Only Author and Title](#)

Givnish, T.J. (1988) Adaptation to sun and shade: a whole-plant perspective. *Functional Plant Biology*, 15, 63–92.

Pubmed: [Author and Title](#)

CrossRef: [Author and Title](#)

Google Scholar: [Author Only Title Only Author and Title](#)

Hikosaka, K. (2016) Optimality of nitrogen distribution among leaves in plant canopies. *Journal of Plant Research*, 129(3), 299–311.

Pubmed: [Author and Title](#)

CrossRef: [Author and Title](#)

Google Scholar: [Author Only Title Only Author and Title](#)

Hirose, T. (2005) Development of the Monsi-Saeki theory on canopy structure and function. *Annals of Botany*, 95, 483–494.

Pubmed: [Author and Title](#)

CrossRef: [Author and Title](#)

Google Scholar: [Author Only Title Only Author and Title](#)

Hubbart, S., Ajigboye, O.O., Horton, P. and Murchie, E.H. (2012) The photoprotective protein PsbS exerts control over CO<sub>2</sub> assimilation rate in fluctuating light in rice. *Plant Journal*, 71, 402–412.

Pubmed: [Author and Title](#)

CrossRef: [Author and Title](#)

Google Scholar: [Author Only Title Only Author and Title](#)

Kromdijk, J., Glowacka, K., Leonelli, L., Gabilly, S.T., Iwai, M., Niyogi, K.K. and Long, S.P. (2016) Improving photosynthesis and crop productivity by accelerating recovery from photoprotection. *Science*, 354(6314), 857–861.

Pubmed: [Author and Title](#)

CrossRef: [Author and Title](#)

Google Scholar: [Author Only Title Only Author and Title](#)

Külheim, C., Agren, J. and Jansson, S. (2002) Rapid regulation of light harvesting and plant fitness in the field. *Science*, 297, 91–93.

Pubmed: [Author and Title](#)

CrossRef: [Author and Title](#)

Google Scholar: [Author Only](#) [Title Only](#) [Author and Title](#)

Lawson, T. and Blatt, M.R. (2014) Stomatal size, speed, and responsiveness impact on photosynthesis and water use efficiency. *Plant Physiology*, 164, 1556–1570.

Pubmed: [Author and Title](#)

CrossRef: [Author and Title](#)

Google Scholar: [Author Only](#) [Title Only](#) [Author and Title](#)

Leakey, A.D.B., Scholes, J.D. and Press, M.C. (2005) Physiological and ecological significance of sunflecks for dipterocarp seedlings. *Journal of Experimental Botany*, 56, 469–82.

Pubmed: [Author and Title](#)

CrossRef: [Author and Title](#)

Google Scholar: [Author Only](#) [Title Only](#) [Author and Title](#)

Lichtenthaler, H.K. (1987) Chlorophylls and carotenoids, the pigments of photosynthetic biomembranes. *Methods in Enzymology*, 148, 350–382.

Pubmed: [Author and Title](#)

CrossRef: [Author and Title](#)

Google Scholar: [Author Only](#) [Title Only](#) [Author and Title](#)

Makino, A. and Osmond, B. (1991) Effects of nitrogen nutrition on nitrogen partitioning between chloroplasts and mitochondria in pea and wheat. *Plant Physiology*, 96, 355–362.

Pubmed: [Author and Title](#)

CrossRef: [Author and Title](#)

Google Scholar: [Author Only](#) [Title Only](#) [Author and Title](#)

Moreau, D., Allard, V., Gaju, O., Le Gouis, J., Foulkes, M.J. and Martre, P. (2012) Acclimation of leaf nitrogen to vertical light gradient at anthesis in wheat is a whole-plant process that scales with the size of the canopy. *Plant Physiology*, 160, 1479–90.

Pubmed: [Author and Title](#)

CrossRef: [Author and Title](#)

Google Scholar: [Author Only](#) [Title Only](#) [Author and Title](#)

Murchie, E.H. and Horton, P. (1997) Acclimation of photosynthesis to irradiance and spectral quality in British plant species: Chlorophyll content, photosynthetic capacity and habitat preference. *Plant, Cell and Environment*, 20, 438–448.

Pubmed: [Author and Title](#)

CrossRef: [Author and Title](#)

Google Scholar: [Author Only](#) [Title Only](#) [Author and Title](#)

Murchie, E.H., Hubbart, S., Chen, Y., Peng, S. and Horton, P. (2002) Acclimation of rice photosynthesis to irradiance under field conditions. *Plant Physiology*, 130, 1999–2010.

Pubmed: [Author and Title](#)

CrossRef: [Author and Title](#)

Google Scholar: [Author Only](#) [Title Only](#) [Author and Title](#)

Murchie, E.H., Hubbart, S., Peng, S. and Horton, P. (2005) Acclimation of photosynthesis to high irradiance in rice: gene expression and interactions with leaf development. *Journal of Experimental Botany*, 56, 449–460.

Pubmed: [Author and Title](#)

CrossRef: [Author and Title](#)

Google Scholar: [Author Only](#) [Title Only](#) [Author and Title](#)

Murchie, E.H. and Reynolds, M.P. (2012) Crop radiation capture and use efficiency. In R.A. Meyers (eds.) *Encyclopedia of Sustainability Science and Technology*. Springer, New York, pp 2615–2638.

Pubmed: [Author and Title](#)

CrossRef: [Author and Title](#)

Google Scholar: [Author Only](#) [Title Only](#) [Author and Title](#)

Niinemets, Ü. and Anten, N. (2009) Packing the photosynthetic machinery: from leaf to canopy. In: Laisk, A., Nedbal, L. and Govindjee (eds.) *Photosynthesis in silico: understanding complexity from molecules to ecosystems*. Dordrecht, Netherlands, pp. 363–399.

Pubmed: [Author and Title](#)

CrossRef: [Author and Title](#)

Google Scholar: [Author Only](#) [Title Only](#) [Author and Title](#)

Niinemets, Ü. and Tenhunen, J.D. (1997) A model separating leaf structural and physiological effects on carbon gain along light gradients for the shade-tolerant species *Acer saccharum*. *Plant, Cell and Environment*, 20, 845–866.

Pubmed: [Author and Title](#)

CrossRef: [Author and Title](#)

Google Scholar: [Author Only](#) [Title Only](#) [Author and Title](#)

Parry, M.A.J., Andralojc, P.J., Parmar, S., Keys, A.J., Habash, D., Paul, M.J., Aired, R., Quick, W.P. and Servaites, J.C. (1997) Regulation of Rubisco by inhibitors in the light. *Plant, Cell and Environment*, 20, 528–534.

Pubmed: [Author and Title](#)

CrossRef: [Author and Title](#)

Google Scholar: [Author Only](#) [Title Only](#) [Author and Title](#)

**Parry, M.A.J., Reynolds, M., Salvucci, M.E., Raines, C., Andralojc, P.J., Zhu, X.-G., Price, G.D., Condon, A.G. and Furbank, R.T. (2010) Raising yield potential of wheat. II. Increasing photosynthetic capacity and efficiency. *Journal of Experimental Botany* 62, 453–467.**

Pubmed: [Author and Title](#)

CrossRef: [Author and Title](#)

Google Scholar: [Author Only](#) [Title Only](#) [Author and Title](#)

**Pask, A.J.D., Sylvester-Bradley, R., Jamieson, P.D. and Foulkes, M.J. (2012) Quantifying how winter wheat crops accumulate and use nitrogen reserves during growth. *Field Crops Research*, 126, 104–118.**

Pubmed: [Author and Title](#)

CrossRef: [Author and Title](#)

Google Scholar: [Author Only](#) [Title Only](#) [Author and Title](#)

**Pearcy, R.W. (1990) Sunflecks and photosynthesis in plant canopies. *Annual Review of Plant Physiology and Plant Molecular Biology*, 41, 421–453.**

Pubmed: [Author and Title](#)

CrossRef: [Author and Title](#)

Google Scholar: [Author Only](#) [Title Only](#) [Author and Title](#)

**Pearcy, R.W. and Seemann, J.R. (1990) Photosynthetic induction state of leaves. *Plant Physiology*, 94, 628–633.**

Pubmed: [Author and Title](#)

CrossRef: [Author and Title](#)

Google Scholar: [Author Only](#) [Title Only](#) [Author and Title](#)

**Poorter, H., Fiorani, F., Pieruschka, R., Wojciechowski, T., Putten, W.H., Kleyer, M., Schurr, U. and Postma, J. (2016) Pampered inside, pestered outside? Differences and similarities between plants growing in controlled conditions and in the field. *New Phytologist*, 212(4), 838-855.**

Pubmed: [Author and Title](#)

CrossRef: [Author and Title](#)

Google Scholar: [Author Only](#) [Title Only](#) [Author and Title](#)

**Pound, M.P., French, A.P., Murchie, E.H. and Pridmore, T.P. (2014) Automated recovery of three-dimensional models of plant shoots from multiple color images. *Plant Physiology*, 166, 1688–1698.**

Pubmed: [Author and Title](#)

CrossRef: [Author and Title](#)

Google Scholar: [Author Only](#) [Title Only](#) [Author and Title](#)

**Powles, S.B. and Björkman, O. (1981) Leaf movement in the shade species *Oxalis oregana*. II. Role in protection against injury by intense light. *Year Book - Carnegie Institution of Washington (USA)*.**

Pubmed: [Author and Title](#)

CrossRef: [Author and Title](#)

Google Scholar: [Author Only](#) [Title Only](#) [Author and Title](#)

**Raven, J.R. (1994) The cost of photoinhibition to plant communities. In: Baker, N.R. and Bowyer, J.R. (eds.) *Photoinhibition of photosynthesis- molecular mechanisms to the field*. Oxford: Bios Sci, pp. 449-464.**

Pubmed: [Author and Title](#)

CrossRef: [Author and Title](#)

Google Scholar: [Author Only](#) [Title Only](#) [Author and Title](#)

**Raven, J.A. (2011) The cost of photoinhibition. *Physiologia Plantarum*, 142(1), 87-104.**

Pubmed: [Author and Title](#)

CrossRef: [Author and Title](#)

Google Scholar: [Author Only](#) [Title Only](#) [Author and Title](#)

**Reich, P.B., Walters, M.B., Ellsworth, D.S., Vose, J.M., Volin, J.C., Gresham, C. and Bowman, W.D. (1998) Relationships of leaf dark respiration to leaf nitrogen, specific leaf area and leaf life-span: a test across biomes and functional groups. *Oecologia*, 114, 471–482.**

Pubmed: [Author and Title](#)

CrossRef: [Author and Title](#)

Google Scholar: [Author Only](#) [Title Only](#) [Author and Title](#)

**Retkute, R., Smith-Unna, S.E., Smith, R.W., Burgess, A.J., Jensen, O.E., Johnson, G.N., Preston, S.P. and Murchie, E.H. (2015) Exploiting heterogeneous environments: does photosynthetic acclimation optimize carbon gain in fluctuating light? *Journal of Experimental Botany*, 66(9), 2437-2447.**

Pubmed: [Author and Title](#)

CrossRef: [Author and Title](#)

Google Scholar: [Author Only](#) [Title Only](#) [Author and Title](#)

**Reynolds, M., Foulkes, M.J., Furbank, R., Griffiths, S., King, J., Murchie, E.H., Parry, M.A.J. and Slafer, G. (2012) Achieving yield gains in wheat. *Plant, Cell & Environment*, 35(10), 1799-1823.**

Pubmed: [Author and Title](#)

CrossRef: [Author and Title](#)

Google Scholar: [Author Only](#) [Title Only](#) [Author and Title](#)

**Sassenrath-Cole, G.F. and Pearcy, R.W. (1994) Regulation of Photosynthetic Induction State by the Magnitude and Duration of Low**

Downloaded from on December 20, 2017 - Published by www.plantphysiol.org

Copyright © 2017 American Society of Plant Biologists. All rights reserved.

**Light Exposure. Plant Physiology, 105(4), 1115–1123.**

Pubmed: [Author and Title](#)

CrossRef: [Author and Title](#)

Google Scholar: [Author Only](#) [Title Only](#) [Author and Title](#)

**Sharkey, T.D., Bernacchi, C.J., Farquhar, G.D. and Singsaas, E.L. (2007) Fitting photosynthetic carbon dioxide response curves for C3 leaves. Plant, Cell and Environment 30:1035-1040.**

Pubmed: [Author and Title](#)

CrossRef: [Author and Title](#)

Google Scholar: [Author Only](#) [Title Only](#) [Author and Title](#)

**Sheue, C.R., Liu, J.W., Ho, J.F., Yao, A.W., Wu, Y.H., Das, S., Tsai, C.C., Chu, H.A, Ku, M.S. and Chesson, P. (2015) A variation on chloroplast development: The bizonoplast and photosynthetic efficiency in the deep-shade plant *Selaginella erythropus*. American Journal of Botany, 102(4), 500-511.**

Pubmed: [Author and Title](#)

CrossRef: [Author and Title](#)

Google Scholar: [Author Only](#) [Title Only](#) [Author and Title](#)

**Sinclair, T.R. and Sheehy, J.E. (1999) Erect leaves and photosynthesis in rice. Science, 283, 1456–1457.**

Pubmed: [Author and Title](#)

CrossRef: [Author and Title](#)

Google Scholar: [Author Only](#) [Title Only](#) [Author and Title](#)

**Song, Q., Zhang, G. and Zhu, X.-G. (2013) Optimal crop canopy architecture to maximise canopy photosynthetic CO<sub>2</sub> uptake under elevated CO<sub>2</sub> – a theoretical study using a mechanistic model of canopy photosynthesis. Functional Plant Biology, 40:109–124**

Pubmed: [Author and Title](#)

CrossRef: [Author and Title](#)

Google Scholar: [Author Only](#) [Title Only](#) [Author and Title](#)

**Stegemann, J., Timm, H.C. and Koppers, M. (1999) Simulation of photosynthetic plasticity in response to highly fluctuating light: an empirical model integrating dynamic photosynthetic induction and capacity. Trees-Structure and Function, 14, 145–160.**

Pubmed: [Author and Title](#)

CrossRef: [Author and Title](#)

Google Scholar: [Author Only](#) [Title Only](#) [Author and Title](#)

**Taylor, S.H. and Long, S.P. (2017) Slow induction of photosynthesis on shade to sun transitions in wheat may cost at least 21% of productivity. Philos. Trans. R. Soc. London B Biol. Sci. 372(1730), 20160543.**

Pubmed: [Author and Title](#)

CrossRef: [Author and Title](#)

Google Scholar: [Author Only](#) [Title Only](#) [Author and Title](#)

**Terashima, I., Araya, T., Miyazawa, S., Sone, K. and Yano, S. (2005) Construction and maintenance of the optimal photosynthetic systems of the leaf, herbaceous plant and tree: an eco-developmental treatise. Annals of Botany, 95, 507–519.**

Pubmed: [Author and Title](#)

CrossRef: [Author and Title](#)

Google Scholar: [Author Only](#) [Title Only](#) [Author and Title](#)

**Terashima, I. and Evans, J.R. (1988) Effects of light and nitrogen nutrition on the organization of the photosynthetic apparatus in spinach. Plant Cell Physiology, 29, 143–155.**

Pubmed: [Author and Title](#)

CrossRef: [Author and Title](#)

Google Scholar: [Author Only](#) [Title Only](#) [Author and Title](#)

**Theobald, J.C., Mitchell, R.A.C., Parry, M.A.J. and Lawlor, D.W. (1998) Estimating the excess investment in Ribulose-1,5-bisphosphate carboxylase/oxygenase in leaves of spring wheat grown under elevated CO<sub>2</sub>. Plant Physiology, 118, 945–955.**

Pubmed: [Author and Title](#)

CrossRef: [Author and Title](#)

Google Scholar: [Author Only](#) [Title Only](#) [Author and Title](#)

**Vialet-Chabrand, S., Matthews, J.S.A., Simkin, A.J., Raines, C.A. and Lawson, T. (2017) Importance of Fluctuations in Light on Plant Photosynthetic Acclimation. Plant Physiology, 173(4), 2163–2179.**

Pubmed: [Author and Title](#)

CrossRef: [Author and Title](#)

Google Scholar: [Author Only](#) [Title Only](#) [Author and Title](#)

**Verhoeven, A.S., Demmig Adams, B. and Adams, W.W. (1997) Enhanced employment of the xanthophyll cycle and thermal energy dissipation in spinach exposed to high light and N stress. Plant Physiology, 113, 817–824.**

Pubmed: [Author and Title](#)

CrossRef: [Author and Title](#)

Google Scholar: [Author Only](#) [Title Only](#) [Author and Title](#)

**Walters, R.G. (2005) Towards an understanding of photosynthetic acclimation. Journal of Experimental Botany, 56, 435–447.**

Pubmed: [Author and Title](#)

CrossRef: [Author and Title](#)

Google Scholar: [Author Only](#) [Title Only](#) [Author and Title](#)



**Watling, J.R., Ball, M.C. and Woodrow, I.E. (1997) The utilization of lightflecks for growth in four Australian rain-forest species. *Functional Ecology*, 11, 231–239.**

Pubmed: [Author and Title](#)

CrossRef: [Author and Title](#)

Google Scholar: [Author Only](#) [Title Only](#) [Author and Title](#)

**Werner, C., Ryel, R.J., Correia, O. and Beyschlag, W. (2001) Effects of photoinhibition on whole-plant carbon gain assessed with a photosynthesis model. *Plant, Cell and Environment*, 24, 27–40.**

Pubmed: [Author and Title](#)

CrossRef: [Author and Title](#)

Google Scholar: [Author Only](#) [Title Only](#) [Author and Title](#)

**Weston, E., Thorogood, K., Vinti, G. and Lopez-Juez, E. (2000) Light quantity controls leaf-cell and chloroplast development in *Arabidopsis thaliana* wild type and blue-light-perception mutants. *Planta*, 211, 807–815.**

Pubmed: [Author and Title](#)

CrossRef: [Author and Title](#)

Google Scholar: [Author Only](#) [Title Only](#) [Author and Title](#)

**Wu, C. (2011) Visual SFM: A visual structure from motion system. Available at: <http://ccwu.me/vsfm>.**

Pubmed: [Author and Title](#)

CrossRef: [Author and Title](#)

Google Scholar: [Author Only](#) [Title Only](#) [Author and Title](#)

**Yamori, W., Masumoto, C., Fukayama, H. and Makino, A. (2012) Rubisco activase is a key regulator of non-steady-state photosynthesis at any leaf temperature and, to a lesser extent, of steady-state photosynthesis at high temperature. *Plant Journal*, 71, 871–880.**

Pubmed: [Author and Title](#)

CrossRef: [Author and Title](#)

Google Scholar: [Author Only](#) [Title Only](#) [Author and Title](#)

**Yin, Z.H. and Johnson, G.N. (2000) Photosynthetic acclimation of higher plants to growth in fluctuating light environments. *Photosynthesis Research*, 63, 97–107.**

Pubmed: [Author and Title](#)

CrossRef: [Author and Title](#)

Google Scholar: [Author Only](#) [Title Only](#) [Author and Title](#)

**Zadoks, J.C., Chang, T.T. and Konzak, C.F. (1974) A decimal code for the growth stages of cereals. *Weed Research*, 14, 415–421.**

Pubmed: [Author and Title](#)

CrossRef: [Author and Title](#)

Google Scholar: [Author Only](#) [Title Only](#) [Author and Title](#)

**Zhu, X.-G., Ort, D., Whitmarsh, J. and Long, S. (2004) The slow reversibility of photosystem II thermal energy dissipation on transfer from high to low light may cause large losses in carbon gain by crop canopies: a theoretical analysis. *Journal of Experimental Botany*, 55, 1167–1175.**

Pubmed: [Author and Title](#)

CrossRef: [Author and Title](#)

Google Scholar: [Author Only](#) [Title Only](#) [Author and Title](#)

**Zhu, X.-G., Long, S.P. and Ort, D.R. (2010) Improving photosynthetic efficiency for greater yield. *Annual Review of Plant Biology*, 61, 235–261.**

Pubmed: [Author and Title](#)

CrossRef: [Author and Title](#)

Google Scholar: [Author Only](#) [Title Only](#) [Author and Title](#)